

# The SPDE approach for spatio-temporal datasets with advection and diffusion

Lucia Clarotto<sup>1\*</sup>, Denis Allard<sup>2†</sup>, Thomas Romary<sup>1†</sup>  
and Nicolas Desassis<sup>1†</sup>

<sup>1\*</sup>Centre for geosciences and geoengineering, Mines Paris, PSL University, Fontainebleau, 77300, France.

<sup>2</sup>Biostatistiques et Processus Spatiaux (BioSP), INRAE, Avignon, 84914, France.

\*Corresponding author(s). E-mail(s):

[lucia.clarotto@minesparis.psl.eu](mailto:lucia.clarotto@minesparis.psl.eu);

†These authors contributed equally to this work.

## Abstract

In the task of predicting spatio-temporal fields in environmental science, introducing models inspired by the physics of the underlying phenomena that are numerically efficient is of growing interest in spatial statistics. The size of space-time datasets calls for new numerical methods to efficiently process them. The SPDE (Stochastic Partial Differential Equation) approach has proven to be effective for the estimation and the prediction in a spatial context. We present here the advection-diffusion SPDE with first order derivative in time to enlarge the SPDE family to the space-time context. By varying the coefficients of the differential operators, the approach allows to define a large class of non-separable spatio-temporal models. A Gaussian Markov random field approximation of the solution of the SPDE is built by discretizing the temporal derivative with a finite difference method (implicit Euler) and by solving the purely spatial SPDE with a finite element method (continuous Galerkin) at each time step. The “Streamline Diffusion” stabilization technique is introduced when the advection term dominates the diffusion term. Computationally efficient methods are proposed to estimate the parameters of the SPDE and to predict the spatio-temporal field by kriging. The approach is applied to a solar radiation dataset. Its advantages and limitations are discussed.

# 1 Introduction

Many areas of environmental science seek to predict a space-time variable of interest from observations at scattered points in the space-time field of study. Among modern techniques proposing efficient methods for estimation and prediction in a spatio-temporal framework, there is a clear distinction between two possible ways of constructing and treating spatio-temporal models (Wikle and Hooten, 2010): either one follows the traditional geostatistical paradigm, using joint space-time covariance functions (see for example Cressie and Huang (1999), Gneiting (2002), Stein (2005)), or one uses dynamical models, by combining time series and spatial statistics (see for example Wikle and Cressie (1999), Sigrist et al. (2012)).

While the theoretical aspects of spatio-temporal geostatistics show good progress (Cressie and Wikle, 2011), implementations lack behind. The geostatistical paradigm can be computationally expensive for large spatio-temporal datasets, due to the factorization of dense  $(N_S N_T, N_S N_T)$  covariance matrices, which is of the order of  $\mathcal{O}((N_S N_T)^3)$ ,  $N_S$  and  $N_T$  being the number of points in space and time respectively. Banerjee et al. (2014) called this issue the “big  $n$  problem”. Moreover, it is hard to define complex space-time covariance functions. For this reason, separable space-time covariance functions have often been applied to spatio-temporal models in order to take advantage of their computational convenience, even when they are not realistic in describing the processes due to the impossibility of allowing space-time interaction in the covariance. Recent studies have focused on constructing non-separable models, which are physically more realistic, albeit computationally more expensive. Non-separable space-time covariance models can be constructed from Fourier transforms of permissible spectral densities, mixtures of separable models, and partial differential equations (PDEs) representing physical laws (Chen et al., 2021; Lindgren et al., 2022). They can be fully symmetric or asymmetric, stationary or non-stationary, univariate or multivariate, and in the Euclidean space or on the sphere. See Porcu et al. (2021) for a recent comprehensive review.

In this paper, we follow the dynamic approach that makes use of physical laws and study models which are defined through Stochastic Partial Differential Equations (SPDEs). The SPDE approach relies on the representation of a continuously indexed Gaussian Field (GF) as a discretely indexed random process, i.e. a Gaussian Markov Random Field (GMRF, see Havard Rue (2005)). Passing from a GF to a GMRF, the covariance function and the dense covariance matrix are substituted respectively by a neighborhood structure and a sparse precision matrix. The advantage of using GMRFs is that the use of sparse precision matrices implies computationally efficient numerical methods, especially for matrix factorization. The link between GF and GMRFs in the purely spatial case has been pioneered by Lindgren et al. (2011), who proposed to construct a GMRF representation of the spatial Matérn field on a triangulated lattice of the domain through the discretization of a diffusion SPDE with a Finite Element Method (FEM). We refer to Bakka (2018) for a

simple explanation of FEM applied to the spatial SPDE or to Section 2.3 for a detailed generalization to spatio-temporal SPDE.

In the spatial framework, major mathematical and algorithmic advances in the SPDE approach have been made (Pereira, 2019; Pereira and Desassis, 2019; Fuglstad et al., 2015), making it possible to efficiently process very large datasets, even in the presence of non-stationarities and varying local anisotropy. The development of SPDE-based approaches to Gaussian processes has led to several practical solutions, among which we find the R package for approximate Bayesian inference R-INLA (Lindgren and Rue, 2015) that uses SPDEs to sample from spatial and separable spatio-temporal models.

When generalizing to the spatio-temporal framework, a direct space-time formulation of the SPDE approach was first suggested in Lindgren et al. (2011), without any precise detail on estimation and prediction methods. The SPDE approach was coupled with the Bayesian framework by Cameletti et al. (2011) to provide a separable space-time model. Non-separable spatio-temporal models have been elaborated in Krainski et al. (2018) and Bakka et al. (2020) as a spatio-temporal generalization of the diffusion-Matérn model of Lindgren et al. (2011).

In all the approaches overviewed above, the space-time processes are symmetrical in the sense that the spatio-temporal covariance does not change when the sign of the space and/or time lag changes. However, atmospheric and geophysical processes are often asymmetric due to transport effects, such as air and water flows. Carrizo-Vergara et al. (2022) defined new spatio-temporal models incorporating the physical processes linked to the studied phenomena (advection, diffusion, etc.). Problems relating to the estimation of the parameters and the conditioning to the observed data remained however open. Sigrist et al. (2015) built non-symmetrical and non-separable space-time Gaussian as a solution to an advection-diffusion SPDE with computationally efficient algorithms for statistical estimation using fast Fourier transforms and Kalman filters. The applicability of this approach remains difficult however, especially in a non-stationary context or with scattered data, as it relies on the Fourier transform of the data. Liu et al. (2020) extended the approach to spatially-varying advection-diffusion and non-zero mean source-sink, leading to a space-time covariance which is non-stationary in space.

In this work, we propose an alternative approach for dealing with spatio-temporal SPDEs that include both a diffusion and an advection terms. In contrast to Sigrist et al. (2015), we make use of the sparse formulation of the spatio-temporal field which is the approximate solution of the SPDE obtained by a combination of FEM and finite differences. This sparse formulation allows to get fast algorithms for parameter estimation and spatio-temporal prediction. We also treat the case of an advection-dominated SPDE, by introducing the Streamline Diffusion stabilization term in the SPDE. We apply our method to a practical dataset of solar irradiance, where a transport effect due to wind is clearly present.

The paper is organized as follows: Section 2 first presents the background of the spatio-temporal SPDE approach, then defines the spatio-temporal advection-diffusion model developed in the paper and its discretization. Moreover, the stabilization of advection-dominated SPDEs is introduced. Section 3 explores fast and scalable estimation methods, kriging formula for prediction and conditional simulations. Section 4 presents an application of the proposed spatio-temporal SPDE approach to a solar radiation dataset. Section 5 discusses the advantages and the limitations of the approach and opens the way to further works on the subject.

## 2 The spatio-temporal advection-diffusion SPDE and its discretization

### 2.1 Background

The spatial SPDE-based approach is a formalism introduced by Lindgren et al. (2011) (from an idea of Whittle (1954, 1963)), that considers the solution  $X(\mathbf{s})$ ,  $\mathbf{s} \in \Omega \subseteq \mathbb{R}^d$ ,  $d$  being the space dimension, of the SPDE

$$(\kappa^2 - \Delta)^{\alpha/2} X(\mathbf{s}) = \tau W(\cdot), \quad (1)$$

where  $\Delta = \sum_{i=1}^d \frac{\partial^2}{\partial s_i^2}$  is the Laplacian operator and  $W(\cdot)$  is a standard spatial Gaussian white noise defined as a (zero-mean) Generalized GRF with the property that the covariance measure of  $W(\cdot)$  over two subregions  $A, B \subseteq \Omega$  is equal to the area measure of their intersection,  $|A \cap B|_\Omega$ . In principle,  $W(\cdot)$  has no element-wise definition, but for a sake of clarity, we will make an abuse of notation and write  $W(\mathbf{s})$ .

Whittle (1954, 1963) showed that  $X(\mathbf{s})$ , solution to Equation (1), is a spatial GF with Matérn covariance

$$C(h) = \frac{\sigma^2}{2^{\nu-1}\Gamma(\nu)} \left(\frac{h}{a}\right)^\nu \mathcal{K}_\nu\left(\frac{h}{a}\right), \quad (2)$$

having regularity parameter  $\nu = \alpha - d/2 > 0$ , scale parameter  $a = \kappa^{-1}$  and variance  $\sigma^2 = \tau^2(4\pi)^{-d/2}\Gamma(\nu)\Gamma(\nu + d/2)^{-1}\kappa^{-2\nu}$ , and where  $h = \|\mathbf{s} - \mathbf{s}'\|$  is the distance between two spatial locations and  $\mathcal{K}_\nu$  is the modified 2<sup>nd</sup> order Bessel function. In particular, when  $\nu = 1/2$  we get the exponential covariance function and when  $\nu \rightarrow +\infty$ , after proper renormalization, we get the Gaussian covariance function.

In Lindgren et al. (2011), the smoothness parameter  $\nu$  considered in the Matérn covariance function corresponds to integer values of  $\alpha$ , hence  $\nu = 0, 1, 2, \dots$  in  $\mathbb{R}^2$ . When non-integer values of  $\nu$  are introduced in the modeling, the SPDE is said to be fractional. A review of results and applications of the fractional SPDE approach is available in Bolin and Kirchner (2020); Roques et al. (2022), but this case will not be treated further in this work.

When generalizing to spatio-temporal processes  $X(\mathbf{s}, t)$ , we consider the general framework proposed in Carrizo-Vergara et al. (2022) for extending the SPDE approach to a wide class of linear spatio-temporal SPDEs. Let us denote  $\boldsymbol{\xi} \in \mathbb{R}^2$  a spatial frequency and  $\omega \in \mathbb{R}$  a temporal frequency. The space-time white noise with unit variance, denoted  $W(\mathbf{s}, t)$ , is characterized by its spectral measure  $d\mu_W(\boldsymbol{\xi}, \omega) = (2\pi)^{-(d+1)/2} d\boldsymbol{\xi} d\omega$ . New spatio-temporal models were obtained from known PDEs describing physical processes, such as diffusion, advection, and oscillations with stochastic forcing terms. In particular, Theorem 1 in Carrizo-Vergara et al. (2022) provides necessary and sufficient conditions to the existence and unicity of stationary solutions to the following general SPDE

$$\left[ \frac{\partial^\beta}{\partial t^\beta} + \mathcal{L}_g \right] X(\mathbf{s}, t) = W_S(\mathbf{s}) \otimes W_T(t). \quad (3)$$

In (3), the spatial operator  $\mathcal{L}_g$  is defined using the spatial Fourier transform on  $\mathbb{R}^2$  (denoted  $\mathcal{F}_S$ ):

$$\mathcal{L}_g(\cdot) = \mathcal{F}_S^{-1}(g\mathcal{F}_S(\cdot)),$$

where  $g : \mathbb{R}^2 \rightarrow \mathbb{C}$  is a sufficiently regular and Hermitian-symmetric function called the *symbol function* of the operator  $\mathcal{L}_g$ . The temporal operator  $\frac{\partial^\beta}{\partial t^\beta}$  is

$$\frac{\partial^\beta}{\partial t^\beta}(\cdot) = \mathcal{F}_T^{-1}((i\omega)^\beta \mathcal{F}_T(\cdot)),$$

where  $\mathcal{F}_T$  is the temporal Fourier transform on  $\mathbb{R}$  and where we have used the symbol function over  $\mathbb{R}$

$$\omega \mapsto (i\omega)^\beta = |\omega|^\beta e^{i \operatorname{sgn}(\omega) \beta \pi / 2}.$$

The spatio-temporal symbol function of the operator involved in (3) is thus

$$(\boldsymbol{\xi}, \omega) \mapsto (i\omega)^\beta + g(\boldsymbol{\xi}) = |\omega|^\beta \cos\left(\frac{\beta\pi}{2}\right) + g_R(\boldsymbol{\xi}) + i \left( \operatorname{sgn}(\omega) |\omega|^\beta \sin\left(\frac{\beta\pi}{2}\right) + g_I(\boldsymbol{\xi}) \right)$$

where  $g_R$  and  $g_I$  are the real and imaginary part of the spatial symbol function  $g(\boldsymbol{\xi})$ . Theorem 1 and Proposition 3 in Carrizo-Vergara et al. (2022) state that (3) admits a unique stationary solution if and only if  $g_R$  is such that  $|g_R|$  is inferiorly bounded by the inverse of a strictly positive polynomial and  $g_R \cos\left(\frac{\beta\pi}{2}\right) \geq 0$ .

## 2.2 The spatio-temporal advection-diffusion SPDE

The advection-diffusion equation is a Partial Differential Equation (PDE) that describes physical phenomena where particles, energy, or other physical quantities evolve inside a physical system due to two processes: diffusion and advection. Advection represents the mass transport due to the average velocity

of all molecules, and diffusion represents the mass transport due to the instantaneously varying velocity of individual molecules, compared to the average velocity of the fluid as a whole.

We here introduce the non-separable space-time models (with  $\mathbf{s} \in \mathbb{R}^2$ ), derived from advection-diffusion SPDEs, i.e., advection-diffusion PDEs where a stochastic noise is added as a forcing term. The model is similar to the one presented in Lindgren et al. (2011), Sigrist et al. (2015), Liu et al. (2020) and Carrizo-Vergara et al. (2022) and reads

$$\left[ \frac{\partial}{\partial t} + \frac{1}{c}(\kappa^2 - \nabla \cdot \mathbf{H} \nabla)^\alpha + \frac{1}{c} \boldsymbol{\gamma} \cdot \nabla \right] X(\mathbf{s}, t) = \frac{\tau}{\sqrt{c}} Z(\mathbf{s}, t), \quad (4)$$

where

- the operator  $\boldsymbol{\gamma} \cdot \nabla$  models the *advection*, where  $\boldsymbol{\gamma} = (\gamma_x, \gamma_y) \in \mathbb{R}^2$  is a velocity vector;
- the operator  $\nabla \cdot \mathbf{H} \nabla$  is a *diffusion* term that can incorporate *anisotropy* in the matrix  $\mathbf{H}$ . When the field is isotropic, i.e.,  $\mathbf{H} = \lambda \mathbf{I}$ , this term reduces to the Laplacian operator  $\lambda \Delta$ ;
- $\kappa^2 > 0$  accounts for *damping*;
- $c$  is a time-scale parameter;
- $\alpha$  is either equal to 1 in presence of diffusion or equal to 0 when there is no diffusion behavior;
- $\tau$  is a standard deviation factor;
- $Z$  is a stochastic forcing term.

Since Equation (4) explicitly models phenomena such as transport and diffusion, the parameters can be given a physical interpretation if desired, but the use of the SPDE is not restricted to situations where it is a priori known that phenomena such as transport and diffusion occur (Sigrist et al., 2015). The stochastic forcing term  $Z(\mathbf{s}, t)$  is assumed separable with

$$Z(\mathbf{s}, t) = W_T(t) \otimes Z_S(\mathbf{s}),$$

where  $Z_S$  is a spatial Generalized Random Field and  $W_T$  is a temporal white noise.  $Z_S$  is often chosen to be a spatial white noise, denoted  $W_S$  in this case. In order to ensure a given regularity for  $Z$ ,  $Z_S$  can alternatively be chosen to be a *colored noise*, such as for example the solution to the spatial Wittle-Matérn SPDE (Lindgren et al., 2011)

$$(\kappa^2 - \nabla \cdot \mathbf{H} \nabla)^{\alpha_S/2} Z_S(\mathbf{s}) = W_S(\mathbf{s}). \quad (5)$$

The spatial dependence of  $Z_S$  ensures a desired regularity of the solutions, and is physically interpreted as a smoothing mechanism for introducing new mass into the system.

**Proposition 1** *Let the coefficients of the SPDE (4) be such that  $\alpha = 0$  and  $\gamma = \mathbf{0}$ ; the spatial operator applied to the spatio-temporal field  $X(\mathbf{s}, t)$  is then the constant value  $c^{-1}$ . Let  $Z(\mathbf{s}, t)$  be a spatio-temporal noise colored in space, with  $Z_S(\mathbf{s})$  satisfying (5). If  $\alpha_S > 1$ , the solution of the SPDE is a separable spatio-temporal field whose covariance is the product of an exponential temporal covariance (with scale parameter equal to  $c$ ) and a Matérn spatial covariance (2) with scale parameter equal to  $a = \kappa^{-1}$ , regularity parameter  $\nu = \alpha_S - 1$  and marginal variance equal to*

$$\sigma^2 = \frac{\tau^2 \Gamma(1/2) \Gamma(\alpha_S - 1)}{\Gamma(1) \Gamma(\alpha_S) 8\pi^{3/2} \kappa^{2(\alpha_S - 1)} |\mathbf{H}|^{1/2}}.$$

In order to get an identifiable model, we will always set  $\mathbf{H}[1, 1] = 1$ . Proposition 1 is a particular case of Corollary 3.3 of Bakka et al. (2020), hence the proof is not reported here.

When  $\alpha = 1$  and  $\gamma$  is non-null,  $X(\mathbf{s}, t)$  is a non-separable spatio-temporal field. The advection-diffusion equation (4) is a particular first order evolution model as in Equation (3) with  $\beta = 1$ . Its spatial symbol function

$$g(\boldsymbol{\xi}) = \frac{1}{c} (\kappa^2 - \boldsymbol{\xi}^\top \mathbf{H} \boldsymbol{\xi} + i \gamma^\top \boldsymbol{\xi}),$$

verifies the necessary and sufficient condition for existence and uniqueness of a stationary solution recalled at the end of Section 2.1. The spatial behavior of this model is described by the spatial SPDE (Carrizo-Vergara et al., 2022)

$$\frac{\sqrt{2}}{c} (\kappa^2 - \nabla \cdot \mathbf{H} \nabla)^{1/2} X_S(\mathbf{s}) = \frac{\tau}{\sqrt{c}} Z_S(\mathbf{s}).$$

**Proposition 2** *Let  $Z(\mathbf{s}, t)$  be a spatio-temporal noise colored in space (such that  $Z_S(\mathbf{s})$  satisfies (5)), and let define  $\alpha_{tot} = \alpha + \alpha_S$ . If  $\alpha_{tot} > 1$ , the spatial trace of the solution  $X(\mathbf{s}, t)$  of the SPDE (4) is a Matérn field with covariance (2) with  $a = \kappa^{-1}$ ,  $\nu = \alpha_{tot} - 1$  and marginal variance  $\sigma^2$  equal to*

$$\sigma^2 = \frac{\tau^2 \Gamma(1/2) \Gamma(\alpha_{tot} - 1)}{\Gamma(1) \Gamma(\alpha_{tot}) 8\pi^{3/2} \kappa^{2(\alpha_{tot} - 1)} |\mathbf{H}|^{1/2}}. \quad (6)$$

A similar proposition, along with its proof, can be found in Proposition 3.1 in Bakka et al. (2020).

## 2.3 Discretization

The advection-diffusion SPDE (4) can be discretized in time and space using a Finite Difference Method (FDM) and a Finite Element Method (FEM), respectively. Since implicit solvers are usually less sensitive to numerical instability than explicit solvers, we choose the implicit Euler scheme for the temporal discretization. This choice prevents errors in the convergence of the algorithm. The FEM method for the spatial discretization is the Continuous Galerkin

method with Neumann Boundary Conditions. This choice is justified in detail in [Lindgren et al. \(2011\)](#).

First, the Implicit Euler scheme is applied to the temporal derivative in order to obtain an approximation of the temporal behavior defined at each time step of the discretization. Let us consider a triangulation  $\mathcal{T}$  of the spatial domain  $\Omega \subset \mathbb{R}^2$  with  $N_S$  vertices  $\{\mathbf{s}_1, \dots, \mathbf{s}_{N_S}\} \subset \mathbb{R}^2$  and define  $h$  the size of the triangulation. Let then consider the purely spatial SPDE defined at each discretization time step. By writing its stochastic weak formulation, we construct a finite element representation  $X_h$  of the solution of the spatial SPDE as a linear combination of piecewise linear basis functions  $\{\psi_i\}_{i=1}^{N_S}$  equal to 1 at the node  $\mathbf{s}_i$  and 0 at all the other nodes, and Gaussian distributed weights  $\{x_i\}_{i=1}^{N_S}$ , such that

$$X_h = \sum_{i=1}^{N_S} x_i \psi_i.$$

The weights determine the values of the field at the vertices, while the values in the interior of the triangles are determined by linear interpolation. The continuous Galerkin finite dimensional solution is obtained by finding the distribution for the representation weights that fulfills the stochastic weak SPDE formulation for the specific set of test functions equal to the basis functions,  $\{\psi_i\}_{i=1}^{N_S}$ .

Given the spatial white noise  $W_S(\mathbf{s})$ , for any set of test functions  $\{\psi_i\}_{i=1}^{N_S}$ , the integrals

$$\int_{\Omega} \psi_i(\mathbf{s}) W_S(\mathbf{s}) d\mathbf{s} \quad i = 1, \dots, N_S$$

are jointly Gaussian, with expectation and covariance measures given by

$$\begin{aligned} \mathbb{E} \left( \int_{\Omega} \psi_i(\mathbf{s}) W_S(\mathbf{s}) d\mathbf{s} \right) &= 0, \\ \text{Cov} \left( \int_{\Omega} \psi_i(\mathbf{s}) W_S(\mathbf{s}) d\mathbf{s}, \int_{\Omega} \psi_j(\mathbf{s}) W_S(\mathbf{s}) d\mathbf{s} \right) &= \int_{\Omega} \psi_i(\mathbf{s}) \psi_j(\mathbf{s}) d\mathbf{s}. \end{aligned}$$

**Proposition 3** *Let  $X(\mathbf{s}, t)$  be the spatio-temporal process of Equation (4) with  $\alpha = 1$  and  $\mathbf{H} = \mathbf{I}$ . Let  $Z(\mathbf{s}, t)$  be a spatio-temporal white noise  $W(\mathbf{s}, t)$ . Let  $\mathcal{T}$  be a triangulation of the spatial domain  $\Omega$  of the process  $X(\mathbf{s}, t)$ . Let  $\{\psi_i\}_{i=1}^{N_S}$  be the piecewise linear basis functions defined over  $\mathcal{T}$ . Finally, let  $\mathbf{M}$  (mass matrix),  $\mathbf{G}$  (stiffness matrix),  $\mathbf{B}$  (advection matrix) and  $\mathbf{K}$  be the  $(N_S, N_S)$  matrices, with entries*

$$\begin{aligned} M_{ij} &= \int_{\Omega} \psi_i(\mathbf{s}) \psi_j(\mathbf{s}) d\mathbf{s}, \\ G_{ij} &= \int_{\Omega} \nabla \psi_i(\mathbf{s}) \cdot \nabla \psi_j(\mathbf{s}) d\mathbf{s}, \\ B_{ij} &= \int_{\Omega} \boldsymbol{\gamma} \cdot \nabla \psi_i(\mathbf{s}) \psi_j(\mathbf{s}) d\mathbf{s}, \\ (K_{\kappa^2})_{ij} &= \kappa^2 M_{ij} + G_{ij}. \end{aligned}$$

Then, the continuous Galerkin finite element solution vector  $\mathbf{x} = \{x_i\}_{i=1}^{N_S}$ , defined on the vertices of the triangulation  $\mathcal{T}$  satisfies at each discretization time step  $(t + dt)$

$$\left( \mathbf{M} + \frac{dt}{c} (\mathbf{K} + \mathbf{B}) \right) \mathbf{x}_{t+dt} = \mathbf{M} \mathbf{x}_t + \frac{\tau \sqrt{dt}}{\sqrt{c}} \mathbf{M}^{1/2} \mathbf{z}_t, \quad (7)$$

where  $\mathbf{z}_t$  is a standard independent Gaussian vector,  $\mathbf{z}_t \sim \mathcal{N}(\mathbf{0}, \mathbf{I})$ , and  $\mathbf{M}^{1/2}$  is any matrix such that  $\mathbf{M}^{1/2} \mathbf{M}^{1/2} = \mathbf{M}$ . When the noise on the right-hand side is colored in space, the discretization reads

$$\left( \mathbf{M} + \frac{dt}{c} (\mathbf{K} + \mathbf{B}) \right) \mathbf{x}_{t+dt} = \mathbf{M} \mathbf{x}_t + \frac{\tau \sqrt{dt}}{\sqrt{c}} \mathbf{L}_S^\top \mathbf{z}_t,$$

where  $\mathbf{L}_S$  is the Cholesky decomposition of the discretized spatial precision matrix  $\mathbf{Q}_S$  of the solution of the spatial SPDE  $(\kappa - \nabla \cdot \mathbf{H} \nabla)^{\alpha_S/2} X_S(\mathbf{s}) = W(\mathbf{s})$ , obtained with the Continuous Galerkin FEM (Lindgren et al., 2011).

*Proof* The proof is available in Appendix A. □

We remark that the elements of the matrices  $\mathbf{M}$ ,  $\mathbf{G}$  and  $\mathbf{B}$  are non-zero only for pairs of basis functions which share common triangles. This implies that the matrix  $(\mathbf{M} + \frac{dt}{c} (\mathbf{K} + \mathbf{B}))$  is sparse and that Equation (7) can be solved by Cholesky decomposition in an efficient way.

## 2.4 Stabilization of advection-dominated SPDE

When the advection term is too important with respect to the diffusion term, we obtain an advection-dominated SPDE. The advection-dominated flow is defined with respect to the Péclet number  $\text{Pe}^h = \frac{\|\gamma\|_h}{2\lambda}$ , where  $\lambda$  is the coefficient of the isotropic Laplacian operator: when  $\text{Pe}^h > 1$ , we are in presence of an advection-dominated flow. When the advection dominates the diffusion, it is well known that the stability of the Finite Element method with the continuous Galerkin method is unsatisfactory (see, for example, Mekuria and Rao (2016) or Quarteroni (2008), Chapter 5). This is due to the fact that the advection term is non-symmetric, and causes the condition number of the matrix  $[\mathbf{M} + \frac{dt}{c} (\mathbf{K} + \mathbf{B})]$  to increase, which leads to oscillations in the solution and may induce instability. A possible solution could be to refine the triangulation until the advection no longer dominates on the element-level. However, in many cases this is not a feasible solution because it would be too much computer demanding. Several stabilization terms can be introduced, some of which are more accurate than others. A detailed explanation of the stabilization approach is reported in Appendix B.

In our case, in the trade-off of order of accuracy and computational complexity, we opt for the Streamline Diffusion stabilization term, that stabilizes the extra advection by introducing an artificial diffusion term along the advection direction.

**Proposition 4** *Let consider the same hypotheses as in Proposition 3. The introduction of the Streamline Diffusion stabilization implies that the discretization defined in Equation (7) becomes*

$$\left( \mathbf{M} + \frac{dt}{c} (\mathbf{K} + \mathbf{B} + \mathbf{S}) \right) \mathbf{x}_{t+dt} = \mathbf{M} \mathbf{x}_t + \frac{\tilde{\tau} \sqrt{dt}}{\sqrt{c}} \mathbf{M}^{1/2} \mathbf{z}_t, \quad (8)$$

where  $\mathbf{S} = [S_{ij}]_{i,j=1}^{N_S}$  is the matrix of the Streamline Diffusion stabilization operator  $\mathcal{S}$ , such that  $S_{ij} = \mathcal{S}(\psi_i, \psi_j) = h|\boldsymbol{\gamma}|^{-1} \int_{\Omega} (\boldsymbol{\gamma} \cdot \nabla \psi_i) (\boldsymbol{\gamma} \cdot \nabla \psi_j) d\mathbf{s}$ , and  $\tilde{\tau} = \tau \left( |\mathbf{H} + h|\boldsymbol{\gamma}|^{-1} \boldsymbol{\gamma} \boldsymbol{\gamma}^\top \right)^{-1/4} (|\mathbf{H}|)^{1/4}$  (see, for example, [Fuglstad et al. \(2015\)](#)). If the noise on the right-hand side of Equation (4) is colored in space, the discretization reads

$$\left( \mathbf{M} + \frac{dt}{c} (\mathbf{K} + \mathbf{B} + \mathbf{S}) \right) \mathbf{x}_{t+dt} = \mathbf{M} \mathbf{x}_t + \frac{\tilde{\tau} \sqrt{dt}}{\sqrt{c}} \mathbf{L}_S^\top \mathbf{z}_t,$$

where  $\mathbf{L}_S$  is the Cholesky decomposition of the discretized spatial precision matrix  $\mathbf{Q}_S$  of the solution of the spatial SPDE  $(\kappa - \nabla \cdot \mathbf{H} \nabla)^{\alpha_S/2} X_S(\mathbf{s}) = W(\mathbf{s})$ , obtained with the Continuous Galerkin FEM ([Lindgren et al., 2011](#)). With this parametrization, the marginal variance of the spatial trace of the field is the same as the one defined in Equation (6) with  $\tilde{\tau}$  instead of  $\tau$ .

The Streamline Diffusion operator  $\mathcal{S}$  can be considered from another point of view as a perturbation of the original SPDE ([Bank et al., 1990](#)). In fact, by making the classical hypothesis of Neumann boundary condition on  $\Omega$  and by using the Green's first identity, we have that

$$\int_{\Omega} (\boldsymbol{\gamma} \cdot \nabla x) (\boldsymbol{\gamma} \cdot \nabla v) d\mathbf{s} = - \int_{\Omega} \nabla \cdot (\boldsymbol{\gamma} \boldsymbol{\gamma}^\top) \nabla x v d\mathbf{s}.$$

This means that the original SPDE (4) can be rewritten with an additional diffusion term as

$$\left[ \frac{\partial}{\partial t} + \frac{1}{c} (\kappa^2 - \nabla \cdot (\mathbf{H} + h|\boldsymbol{\gamma}|^{-1} \boldsymbol{\gamma} \boldsymbol{\gamma}^\top) \nabla + \boldsymbol{\gamma} \cdot \nabla) \right] X(\mathbf{s}, t) = \frac{\tilde{\tau}}{\sqrt{c}} Z(\mathbf{s}, t). \quad (9)$$

The term  $(h|\boldsymbol{\gamma}|^{-1} \boldsymbol{\gamma} \boldsymbol{\gamma}^\top)$  acts as an anisotropic “diffusion” tensor that is added to the anisotropy (or identity) matrix  $\mathbf{H}$  of the original diffusion. This extra diffusion stabilizes the advection directed along the direction  $\boldsymbol{\gamma}$ .

## 2.5 Spatio-temporal Gaussian Markov Random Field approximation

**Proposition 5** *In presence of an advection-dominated flow and a spatio-temporal white noise on the right-hand side of Equation (4), the discretized vector  $\mathbf{x}_{t+dt}$  on the mesh  $\mathcal{T}$  at each time step can be found as the solution of the following equation:*

$$\begin{aligned} \mathbf{x}_0 &\sim \mathcal{N}(\mathbf{0}, \boldsymbol{\Sigma}_0), \\ \mathbf{x}_{t+dt} &= \mathbf{D} \mathbf{x}_t + \mathbf{E} \mathbf{z}_t, \end{aligned} \quad (10)$$

where

$$\begin{aligned}\mathbf{D} &= (\mathbf{M} + \frac{dt}{c}(\mathbf{K} + \mathbf{B} + \mathbf{S}))^{-1} \mathbf{M}, \\ \mathbf{E} &= \frac{\tilde{\tau}\sqrt{dt}}{\sqrt{c}}(\mathbf{M} + \frac{dt}{c}(\mathbf{K} + \mathbf{B} + \mathbf{S}))^{-1} \mathbf{M}^{1/2},\end{aligned}\tag{11}$$

and  $\mathbf{z}_t \sim \mathcal{N}(\mathbf{0}, \mathbf{I})$  is independent of  $\mathbf{x}_0, \dots, \mathbf{x}_t$ . In presence of a spatio-temporal noise colored in space on the right-hand side of Equation (4), the matrix  $\mathbf{E}$  reads

$$\mathbf{E} = \frac{\tilde{\tau}\sqrt{dt}}{\sqrt{c}}(\mathbf{M} + \frac{dt}{c}(\mathbf{K} + \mathbf{B} + \mathbf{S}))^{-1} \mathbf{L}_S^\top,$$

with  $\mathbf{L}_S$  defined in Proposition 4.

*Proof* Starting from Equation (8), which represents the numerical scheme for the advection-diffusion spatio-temporal SPDE with stabilization, it is straightforward to obtain (10).  $\square$

When the SPDE is not advection-dominated (and hence no stabilization term is needed), Equation (11) is replaced by the similar equation where the matrix  $\mathbf{S}$  is deleted and where  $\tilde{\tau}$  is replaced by  $\tau$ .

The covariance matrix  $\Sigma_0$  can be taken to be equal to any admissible positive definite matrix. The speed of convergence to the stationary solution of the equation will depend on the proximity of the covariance of the spatial trace of  $X(\mathbf{s}, t)$  to  $\Sigma_0$ . When the noise is colored in space, we can set  $\Sigma_0$  to be equal to the Matérn covariance of the spatial trace defined in Proposition 2.

To make the precision matrix sparse to obtain GMRF models,  $\mathbf{M}$  should be replaced by the diagonal matrix  $\tilde{\mathbf{M}}$ , where  $\tilde{\mathbf{M}}_{ii} = \langle \psi_i, 1 \rangle$ . This technique is called mass lumping and is common practice in FEM. From now on, we always use the lumped matrix  $\tilde{\mathbf{M}}$ , but for ease of reading, it will still be denoted  $\mathbf{M}$ .

**Proposition 6** Let us denote  $\mathbf{x}_{0:t} = [\mathbf{x}_0, \dots, \mathbf{x}_t]^\top$  the vector containing all spatial solutions until time step  $t$ , the global precision matrix  $\mathbf{Q}$  of the vector  $\mathbf{x}_{0:t}$  reads

$$\mathbf{Q} = \begin{pmatrix} \Sigma_0^{-1} + \mathbf{D}^\top \mathbf{F}^{-1} \mathbf{D} & -\mathbf{D}^\top \mathbf{F}^{-1} & 0 & \dots & 0 \\ -\mathbf{F}^{-1} \mathbf{D} & \mathbf{F}^{-1} + \mathbf{D}^\top \mathbf{F}^{-1} \mathbf{D} - \mathbf{D}^\top \mathbf{F}^{-1} & \ddots & \ddots & \vdots \\ \vdots & \ddots & \ddots & \ddots & 0 \\ \vdots & \ddots & -\mathbf{F}^{-1} \mathbf{D} & \mathbf{F}^{-1} + \mathbf{D}^\top \mathbf{F}^{-1} \mathbf{D} - \mathbf{D}^\top \mathbf{F}^{-1} & \vdots \\ 0 & \dots & 0 & -\mathbf{F}^{-1} \mathbf{D} & \mathbf{F}^{-1} \end{pmatrix},\tag{12}$$

where  $\mathbf{F} = \mathbf{E} \mathbf{E}^\top$ .

*Proof* The proof is available in Appendix C.  $\square$

### 3 Estimation, prediction and simulation

This section explores the techniques for estimation and prediction of spatio-temporal processes following the SPDE approach described in Section 2. We will consider the SPDE (4) with  $\alpha = 1$ ,  $\mathbf{H} = \mathbf{I}$  (isotropic diffusion) and colored noise in space with  $\alpha_S = 2$ . Similar computations can be generalized to other values of  $\alpha_S$  such that  $\alpha_S/2$  is integer or to anisotropic diffusion.

We consider  $n$  spatio-temporal data  $\mathbf{z}$  scattered in the spatio-temporal domain  $\Omega \times [0, T]$ , discretized in space with a triangulation  $\mathcal{T}$  with  $N_S$  nodes and discretized in time by means of  $N_T$  regular time steps. We shall denote this space-time discretization  $\mathcal{T}' = \mathcal{T} \times \{1/T, \dots, N_T/T\}$ . We assume a statistical model with fixed and random effects. The fixed effect is a regression on a set of covariates and the random effect is modeled as the FEM discretization of a random field described by the SPDE (4) with the addition of random noise:

$$\mathbf{z} = \boldsymbol{\eta} \mathbf{b} + \mathbf{A}^\top \mathbf{x} + \sigma_0 \boldsymbol{\varepsilon}, \quad (13)$$

where  $\mathbf{b}$  is the vector of  $q$  fixed effects and  $\boldsymbol{\eta}$  is a  $(n, q)$  matrix of covariates with  $[\boldsymbol{\eta}]_{jk} = \eta_k(\mathbf{s}_j, t_j)$ ,  $j = 1, \dots, n$  and  $k = 1, \dots, q$ . The matrix  $\mathbf{A}$  is the  $(N_S N_T, n)$  projection matrix between the points in  $\mathcal{T}'$  and the data, and  $\boldsymbol{\varepsilon}$  is a standard Gaussian random vector with independent components.

#### 3.1 Estimation of the parameters

The parameters of the SPDE are estimated using Maximum Likelihood (ML). We collect the parameters of the SPDE in the vector  $\boldsymbol{\theta}^\top = (\kappa, \gamma_x, \gamma_y, c, \tau)$ , while the parameters of the statistical model are collected in  $\boldsymbol{\psi}^\top = (\boldsymbol{\theta}^\top, \mathbf{b}^\top, \sigma_0)$ . Following (13),  $\mathbf{z}$  is a Gaussian vector with expectation  $\boldsymbol{\eta} \mathbf{b}$  and covariance matrix

$$\boldsymbol{\Sigma}_{\mathbf{z}} = \mathbf{A}^\top \mathbf{Q}^{-1}(\boldsymbol{\theta}) \mathbf{A} + \sigma_0^2 \mathbf{I}_{(n, n)},$$

where  $\mathbf{Q}(\boldsymbol{\theta})$  is a precision matrix of size  $(N_S N_T, N_S N_T)$  depending on the parameters  $\boldsymbol{\theta}$ . For ease of notation, we use  $\mathbf{Q}$  instead of  $\mathbf{Q}(\boldsymbol{\theta})$ . The log-likelihood is equal to

$$\mathcal{L}(\boldsymbol{\psi}) = -\frac{n}{2} \log(2\pi) - \frac{1}{2} \log|\boldsymbol{\Sigma}_{\mathbf{z}}(\boldsymbol{\psi})| - \frac{1}{2} (\mathbf{z} - \boldsymbol{\eta} \mathbf{b})^\top \boldsymbol{\Sigma}_{\mathbf{z}}^{-1}(\boldsymbol{\psi}) (\mathbf{z} - \boldsymbol{\eta} \mathbf{b}). \quad (14)$$

We use the Broyden, Fletcher, Goldfarb, and Shanno (BFGS) optimization algorithm, that makes use of the second-order derivative of the objective function. The gradients of the log-likelihood function (14) with respect to the different parameters included in  $\boldsymbol{\psi}$  are approximately computed with a Finite Difference Method.

We now propose an easier formulation of each term of the profile log-likelihood (14) to speed up the computations. Concerning the term  $\log|\boldsymbol{\Sigma}_{\mathbf{z}}|$  we derive the following property:

**Proposition 7** *In the framework outlined above, we have*

$$\log|\Sigma_{\mathbf{z}}| = n \log \sigma_0^2 - \log|\mathbf{Q}| + \log|\mathbf{Q} + \sigma_0^{-2} \mathbf{A} \mathbf{A}^\top|. \quad (15)$$

*Proof* To compute  $\log|\Sigma_{\mathbf{z}}|$ , let us consider the augmented matrix

$$\Sigma_c = \begin{pmatrix} \mathbf{Q}^{-1} & \mathbf{Q}^{-1} \mathbf{A} \\ \mathbf{A}^\top \mathbf{Q}^{-1} & \Sigma_{\mathbf{z}} \end{pmatrix}. \quad (16)$$

By using block formulas, we have

$$\log|\Sigma_c| = -\log|\mathbf{Q}| + n \log \sigma_0^2,$$

and

$$\log|\Sigma_c| = \log|\Sigma_{\mathbf{z}}| + \log|\mathbf{Q}^{-1} - \mathbf{Q}^{-1} \mathbf{A} \Sigma_{\mathbf{z}}^{-1} \mathbf{A}^\top \mathbf{Q}^{-1}| = \log|\Sigma_{\mathbf{z}}| - \log|\mathbf{Q} + \sigma_0^{-2} \mathbf{A} \mathbf{A}^\top|,$$

where the last equality is a consequence of the Woodbury identity. This leads to the result.  $\square$

**Proposition 8** *The term  $\log|\mathbf{Q}|$  of Equation (15) can be computed with the computationally cheap formula*

$$\log|\mathbf{Q}| = \log|\Sigma_0^{-1}| + (N_T - 1) \log|\mathbf{F}^{-1}|, \quad (17)$$

where  $N_T$  is the number of time steps and  $\mathbf{F}^{-1} = \frac{c}{\bar{\tau}^2 dt} (\mathbf{M} + \frac{dt}{c} (\mathbf{K} + \mathbf{B} + \mathbf{S}))^\top \mathbf{M}^{-1} (\mathbf{M} + \frac{dt}{c} (\mathbf{K} + \mathbf{B} + \mathbf{S}))$ .  $\mathbf{M}^{-1}$  is replaced by  $\mathbf{Q}_S$  when the noise is colored in space.  $|\mathbf{F}^{-1}|$  is the determinant of an  $(N_S, N_S)$  sparse, symmetric and positive definite matrix. The computation of its determinant can be obtained by Cholesky decomposition of  $\mathbf{F}^{-1}$ .

*Proof* Following Powell (2011), let  $\mathbf{N}_N = [\mathbf{N}_{ij}]_{i,j=1}^N$  be an  $(nN, nN)$  matrix, which is partitioned into  $N$  blocks, each of size  $(n, n)$ . Then the determinant of  $\mathbf{N}_N$  is

$$|\mathbf{N}_N| = \prod_{k=1}^N |\alpha_{kk}^{(N-k)}|,$$

where the  $\alpha^{(k)}$  are defined by

$$\begin{aligned} \alpha_{ij}^{(0)} &= \mathbf{N}_{ij} \\ \alpha_{ij}^{(k+1)} &= \alpha_{ij}^{(k)} - \alpha_{i, N-k}^{(k)} (\alpha_{N-k, N-k}^{(k)})^{-1} \alpha_{N-k, j}^{(k)}, \quad k \geq 1. \end{aligned}$$

$\mathbf{Q}$  is a block-matrix organized as  $\mathbf{N}_N$ . Hence, the formula for  $|\mathbf{Q}|$  is

$$|\mathbf{Q}| = |\Sigma_0^{-1}| |\mathbf{F}^{-1}|^{N-1}. \quad (18)$$

Applying the logarithm, we obtain Equation (17).  $\square$

The term  $\log|\mathbf{Q} + \sigma_0^{-2} \mathbf{A} \mathbf{A}^\top|$  must be analyzed in detail. The term  $\sigma_0^{-2} \mathbf{A} \mathbf{A}^\top$  is an  $(N_S N_T, N_S N_T)$  diagonal block matrix, whose  $(N_S, N_S)$  blocks are sparse. The computation of  $\log|\mathbf{Q} + \sigma_0^{-2} \mathbf{A} \mathbf{A}^\top|$  is not straightforward as in the case of  $\log|\mathbf{Q}|$ , since there is no way of reducing the computation to purely spatial matrices. Depending on the size  $N_S N_T$ , we can either apply a Cholesky

decomposition of the  $(N_S N_T, N_S N_T)$  matrix  $(\mathbf{Q} + \sigma_0^{-2} \mathbf{A} \mathbf{A}^\top)$  or a matrix-free approach that is detailed below.

When the number of mesh points prevents us from computing the Cholesky decomposition of  $(\mathbf{Q} + \sigma_0^{-2} \mathbf{A} \mathbf{A}^\top)$ , we can approximate  $\log|\mathbf{Q} + \sigma_0^{-2} \mathbf{A} \mathbf{A}^\top|$  by expressing it as  $\text{tr}[\log(\mathbf{Q} + \sigma_0^{-2} \mathbf{A} \mathbf{A}^\top)]$ , approximating the log function with a Chebyshev polynomial and using the Hutchinson's estimator (Hutchinson, 1990) to obtain a stochastic estimate of the trace of the matrix  $[\log(\mathbf{Q} + \sigma_0^{-2} \mathbf{A} \mathbf{A}^\top)]$ . The method is detailed in Algorithm 5 of Pereira et al. (2022).

Concerning the computation of the quadratic term of the log-likelihood, we note that using the Woodbury formula again, we can work with the more convenient expression

$$\Sigma_{\mathbf{z}}^{-1} = \sigma_0^{-2} \mathbf{I}_{(n,n)} - \sigma^{-4} \mathbf{A}^\top (\mathbf{Q} + \sigma_0^{-2} \mathbf{A} \mathbf{A}^\top)^{-1} \mathbf{A}$$

that leads to the formula

$$\begin{aligned} (\mathbf{z} - \boldsymbol{\eta} \mathbf{b})^\top \Sigma_{\mathbf{z}}^{-1} (\psi) (\mathbf{z} - \boldsymbol{\eta} \mathbf{b}) &= \sigma_0^{-2} (\mathbf{z} - \boldsymbol{\eta} \mathbf{b})^\top \mathbf{I}_{(n,n)} (\mathbf{z} - \boldsymbol{\eta} \mathbf{b}) + \\ &\quad - \sigma_0^{-4} (\mathbf{z} - \boldsymbol{\eta} \mathbf{b})^\top \mathbf{A}^\top (\mathbf{Q} + \sigma_0^{-2} \mathbf{A} \mathbf{A}^\top)^{-1} \mathbf{A} (\mathbf{z} - \boldsymbol{\eta} \mathbf{b}), \end{aligned}$$

which is obtained by first computing the second term either by Cholesky decomposition or with the Conjugate Gradient method. This latter method solves  $\mathbf{N} \mathbf{v} = \mathbf{w}$  with respect to  $\mathbf{v}$  and computes  $\mathbf{v}_{sol} = \mathbf{w}^\top \mathbf{v}$ , with  $\mathbf{N} = (\mathbf{Q} + \sigma_0^{-2} \mathbf{A} \mathbf{A}^\top)$  and  $\mathbf{w} = \mathbf{A} (\mathbf{z} - \boldsymbol{\eta} \mathbf{b})$ . In this case, it is useful to find a good preconditioner for the matrix  $(\mathbf{Q} + \sigma_0^{-2} \mathbf{A} \mathbf{A}^\top)$  to ensure fast convergence of the conjugate gradient method. A temporal block Gauss-Seidel preconditioner is a good choice in this case. A detailed explanation of the Conjugate Gradient method and the Gauss-Seidel preconditioner is available in Appendix D.

In Table 1 we report some results of estimation of the parameters  $\boldsymbol{\theta}^\top = (\kappa, \gamma_x, \gamma_y, c, \tau)$  for a spatio-temporal model simulated with the SPDE (4). We set  $\mathbf{H} = \mathbf{I}$ ,  $\alpha = 1$ ,  $\alpha_S = 2$  and the other parameters of the spatio-temporal discretization to the following:  $N_S = 900$ ,  $dx = dy = 1$ ,  $dt = 1$ ,  $N_T = 10$  and  $n_S = 500$  observations in the spatial domain at the same locations for the  $N_T$  time-steps (hence  $n = 5000$ ). Since the size of both the dataset and the spatio-temporal mesh is quite small, we report only the estimations computed with the Cholesky decomposition.

The initial values for the estimation have been set in the following way: first, a Matérn variogram with regularity parameter fixed at  $\nu = \alpha + \alpha_S - 1 = 2$  is fitted to one (or more) spatial trace of data in order to set the value of  $\kappa$  equal to  $\kappa = \sqrt{12\nu}/r_M$ , where  $r_M$  is the practical range (the distance at which the correlation is approximately equal to 0.05), and the value of  $\sigma^2$  equal to the sill. Then an exponential variogram is fitted to the temporal trace and  $c$  is set to be equal to  $c = r_E/3$ , where  $r_E$  is the practical range of the exponential variogram. In other words, we initialize the parameters of the SPDE model to the values obtained through the method of moments applied assuming the

hypothesis of Proposition 2. Finally  $\gamma$  is set to  $\gamma = \mathbf{0}$ , i.e., to the purely diffusive case.

$\kappa$	$\hat{\kappa}$	$\gamma_x$	$\hat{\gamma}_x$	$\gamma_y$	$\hat{\gamma}_y$	$c$	$\hat{c}$	$\tau$	$\hat{\tau}$	average time (s)
0.2	0.203 (0.051)	-2	-2.043 (0.262)	3	2.979 (0.351)	1	1.037 (0.093)	1	1.036 (0.092)	120
0.33	0.328 (0.059)	-1	-1.008 (0.134)	1	1.018 (0.143)	0.5	0.546 (0.041)	1.2	1.221 (0.037)	124

**Table 1** Mean (and standard deviation) of ML estimates  $\hat{\theta}^\top = (\hat{\kappa}, \hat{\gamma}_x, \hat{\gamma}_y, \hat{c}, \hat{\tau})$  over 10 simulations for two different subsets of advection-diffusion model's parameters

## 3.2 Kriging

From the vector  $\mathbf{z}$  of data at the observed locations defined in Equation (13), we aim to predict of the spatio-temporal vector  $\mathbf{x}$  on the entire spatial mesh during the time window  $[0, T]$ , i.e. on  $\mathcal{T}'$ . The prediction is made through kriging, which computes the conditional expectation of  $\mathbf{x}$  knowing  $\mathbf{z}$  as

$$\mathbf{x}^* = \mathbb{E}(\mathbf{x}|\mathbf{z}) = (\mathbf{Q} + \sigma_0^{-2} \mathbf{A} \mathbf{A}^\top)^{-1} \mathbf{A} \mathbf{z}. \quad (19)$$

This formula comes from the definition of the augmented matrix  $\Sigma_c$  of equation (16). The computation of (19) requires the inversion of the  $(N_S N_T, N_S N_T)$  matrix  $(\mathbf{Q} + \sigma_0^{-2} \mathbf{A} \mathbf{A}^\top)^{-1}$ , that can be achieved by Cholesky decomposition or Conjugate Gradient method as explained in Section 3.1. The conditional variance, also called kriging variance, is

$$\text{Var}(\mathbf{x}|\mathbf{z}) = (\mathbf{Q} + \sigma_0^{-2} \mathbf{A} \mathbf{A}^\top)^{-1}.$$

The extrapolation of the diagonal of an inverse matrix is not straightforward when only the Cholesky decomposition of the matrix is available. Some methods exist to as the Takahashi method described in Takahashi et al. (1973) and Erismann and Tinney (1975). Another way of computing the kriging variance is through conditional simulations, as will be detailed in Section 3.3.

If we want to predict the  $(N_S)$  vector  $\mathbf{x}_{T+1}$  at time  $(T+1)$  on the mesh, we can define  $\mathbf{x}_{T+1}$  using a time discretization step as defined in Equation (10)

$$\mathbf{x}_{T+1} = \mathbf{D} \mathbf{x}_T + \mathbf{E} \varepsilon_{T+1},$$

where  $\mathbf{x}_T$  is the last subset of size  $(N_S)$  of vector  $\mathbf{x}$  related to time  $T$  and  $\varepsilon_{T+1}$  is a  $(N_S)$  standardized Gaussian vector. If we want to link  $\mathbf{x}_{T+1}$  to  $\mathbf{x}$  (the vector containing all time steps), we must replace the  $(N_S, N_S)$  matrix  $\mathbf{D}$  with a sparse  $(N_S, N_S N_T)$  matrix  $\mathbf{D}_{ST}$  with  $N_T$  blocks, all of whom are null except the last  $(N_S, N_S)$  block, which is equal to  $\mathbf{D}$ . The same procedure is done for  $\mathbf{E}$ . Hence, we obtain

$$\mathbf{x}_{T+1} = \mathbf{D}_{ST} \mathbf{x} + \mathbf{E}_{ST} \varepsilon_{ST},$$

where  $\varepsilon_{ST}$  is a  $(N_S N_T)$  standardized Gaussian vector. The covariance between  $\mathbf{x}_{T+1}$  and  $\mathbf{z}$  (the  $(n)$  observation vector) is then given by  $\mathbf{D}_{ST} \mathbf{Q}^{-1} \mathbf{A}$ . If we consider the augmented covariance matrix  $\Sigma_{c+1}$  of the vectors  $\mathbf{x}$ ,  $\mathbf{x}_{T+1}$  and  $\mathbf{z}$ , we have

$$\Sigma_{c+1} = \begin{pmatrix} \mathbf{Q}^{-1} & \mathbf{Q}^{-1} \mathbf{D}_{ST}^\top & \mathbf{Q}^{-1} \mathbf{A} \\ \mathbf{D}_{ST} \mathbf{Q}^{-1} & \mathbf{D}_{ST} \mathbf{Q}^{-1} \mathbf{D}_{ST}^\top + \mathbf{E}_{ST} \mathbf{E}_{ST}^\top & \mathbf{D}_{ST} \mathbf{Q}^{-1} \mathbf{A} \\ \mathbf{A}^\top \mathbf{Q}^{-1} & \mathbf{A}^\top \mathbf{Q}^{-1} \mathbf{D}_{ST}^\top & \Sigma_{\mathbf{z}} \end{pmatrix}.$$

Finally, we obtain the formula for kriging  $\mathbf{x}_{T+1}^*$  at  $(T+1)$  as

$$\mathbf{y}_{T+1}^* = \mathbb{E}(\mathbf{y}_{T+1} | \mathbf{z}) = \mathbf{D}_{ST} (\mathbf{Q} + \sigma_0^{-2} \mathbf{A} \mathbf{A}^\top)^{-1} \mathbf{A} \mathbf{z}. \quad (20)$$

This formula means that we can obtain the kriging  $\mathbf{x}_{T+1}^*$  at time  $(T+1)$  just by applying one Implicit Euler step to the kriging result  $\mathbf{x}_{T+1}^*$  at time  $T$ . The same procedure can be used to predict at time  $(T+2)$  and so on.

### 3.3 Conditional simulations

To realize a conditional simulation, we use the conditional kriging paradigm detailed below. First we realize a non-conditional simulation  $\mathbf{x}_{NC}$  on the spatio-temporal grid  $\mathcal{T}'$ . At the observation points  $(\mathbf{s}, t) \in \mathcal{I}$ , we compute the vector  $\mathbf{z}_{\mathcal{I}}$

$$\mathbf{z}_{\mathcal{I}} = \mathbf{A}^\top \mathbf{x}_{NC} + \varepsilon.$$

We define the residuals as  $\mathbf{r}_{\mathcal{I}} = \mathbf{z}_{\mathcal{I}} - \mathbf{x}_{NC}(\mathcal{I})$ , where the last term represents  $\mathbf{x}_{NC}$  considered at the observation locations only. Then we apply kriging on the residuals and obtain the values  $\mathbf{r}^*$  over the entire spatio-temporal grid  $\mathcal{T}'$ ; we here use the method explained in Section 3.2. Finally, the conditional simulation is obtained as

$$\mathbf{z}_C(\mathcal{I}) = \mathbf{A}^\top \mathbf{x}_{NC} + \mathbf{A}^\top \mathbf{r}^*.$$

## 4 Application to a solar radiation dataset

The approach detailed in the previous sections is now applied to a solar radiation dataset for which experts agree on the presence of advection due to Western prevailing winds transporting the clouds from one side of the domain to the other. The HOPE campaign (Macke et al., 2017) recorded Global Horizontal Irradiance (GHI) (or SSI, Surface Solar Irradiance) over a  $10000 \times 16000 \text{ m}^2$  region in West Germany near the city of Jülich from the 2nd of April, to the second of July, 2013. The sensors were located at 99 stations located as pictured in Figure 1 and GHI was recorded every 15 seconds. A detailed description of the campaign can be found in Macke et al. (2017).

The dataset was cleaned for outlying values and non-operating sensors, and the temporal resolution was reduced from 15 seconds to 1 minute. Figure 2

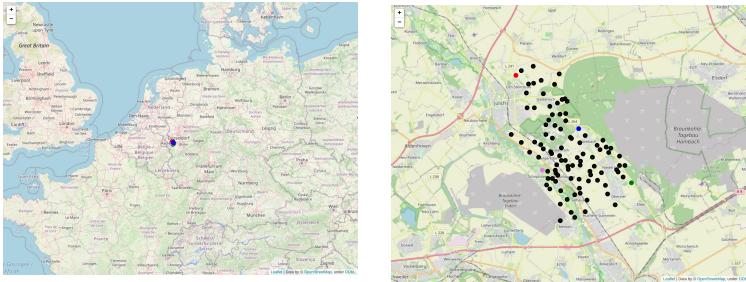


**Fig. 1** Stations over the spatial domain

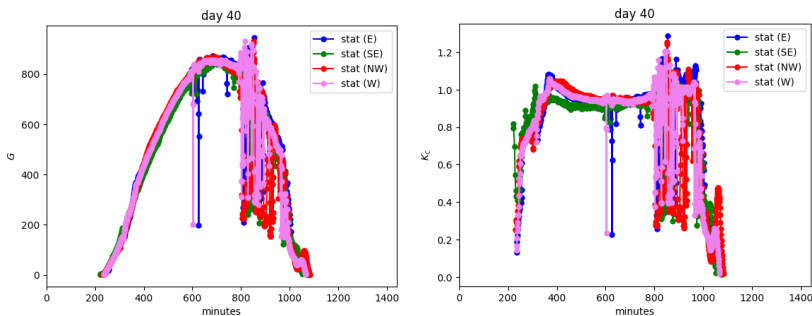


**Fig. 2** GHI  $G$  and Clear Sky Index  $K_c$  for 4 different stations on the 28th of May 2013

(left panel) shows GHI as a function of time (in minute, during a full day – the 28th of May 2013) at 4 different stations. These stations, represented in color in Figure 1, are located at the border of the domain, far from each other. The GHI starts close to 0, increases after sunrise, peaks at midday and tends to 0 at sunset. The maximal theoretical amount of irradiance reaching the sensor follows an ideal concave curve. The divergence between the measured irradiance and the optimal curve can be slight or important, depending on the presence of clouds. One can see on this example that the evolution among the 4 stations is similar, with variations accounting for spatio-temporal variations of the clouds.

A first preprocessing was made in order to stationarize the phenomenon. Oumbe et al. (2014) showed that the solar irradiance at ground level, GHI (denoted  $G$  for short from now on), computed by a radiative transfer model can be approximated by the product of the irradiance under clear atmosphere (called Clear Sky GHI, or  $G_c$ ) and a modification factor due to cloud properties and ground albedo only (Clear Sky Index, or  $K_c$ , Beyer et al. (1996)):

$$G \simeq G_c K_c. \quad (21)$$

The error made in using this approximation depends mostly on the solar zenith angle, the ground albedo and the cloud optical depth. In most cases, the maximum errors (95th percentile) on global and direct surface irradiances are less

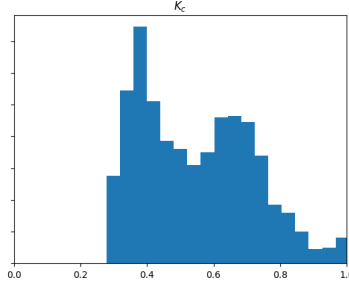


**Fig. 3** Histogram of GHI over 20 time steps

than  $15 \text{ Wm}^{-2}$  and less than 2- to 5 % in relative value, as recommended by the World Meteorological Organization for high-quality measurements of the solar irradiance (Oumbe et al., 2014). Practically, it means that a model for fast calculation of surface solar irradiance may be separated into two distinct and independent models: i) a deterministic model for  $G$ , under clear-sky conditions, as computed according to Gschwind et al. (2019), considered as known in this study; ii) a model for  $K_c$  which accounts for cloud influence on the downwelling radiation and is expected to change in time and space.  $K_c$  is modeled as a random spatio-temporal process and will be the subject of our analysis. Figure 2 (right panel) shows the variable  $K_c$  at the same 4 stations and on the same day of left panel. In general,  $K_c$  lies between 0 and 1, but in rare occasions, values above 1 can be observed. This phenomenon is called *overshooting* (Schade et al., 2007).

#### 4.1 Estimation and prediction

As an example of application of the estimation and prediction methods described in Section 3, we extract a time window of 16 minutes around 4 p.m. the 28th of May 2013 and we consider observations every minute at the 73 stations with well recorded values. We compute the spatial prediction by kriging on a fine grid over the  $T = 16$  time steps and the spatio-temporal prediction at the two following minutes:  $(T + 1)$  and  $(T + 2)$ . The estimation of the SPDE parameters is done according to the method described in Section 3.1. Kriging equations are computed as presented in Section 3.2 for the 16 time steps on a grid of 900 points. Results are shown in Figure 4 for the last five minutes (from  $t = 12$  to  $t = 16$ ). To assess the accuracy of the predictions in the direction of the prevailing winds, we apply the kriging procedure to a restricted dataset where a subset of observations in the South-Eastern region has been removed. The kriging formulae are then computed with a subset of observations. The two step-ahead predictions are made by applying the Implicit Euler discretization scheme to the kriging vector at time  $T$  as presented at the end of Section 3.2. Prediction maps at time  $T$ ,  $(T + 1)$  and  $(T + 2)$  are plotted in the upper panel of Figure 5, along with the correct values with black outline. In the lower panel, we plot the signed error ( $\text{Real } K_c - \text{Pred } K_c$ ).

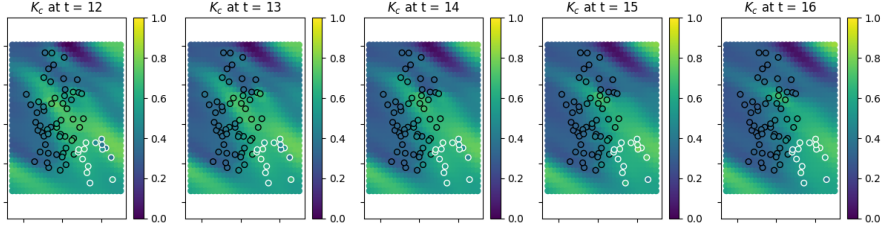


**Fig. 4** Kriging of  $K_c$  over the last 5 time steps. The points with black outline are the real values of  $K_c$

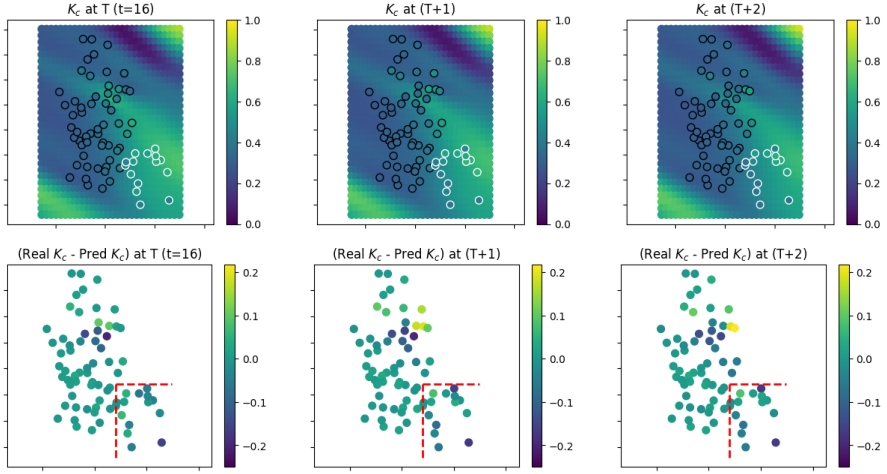


**Fig. 5** High: Predicted kriging of  $K_c$  at  $T$ ,  $(T + 1)$  and  $(T + 2)$ . The points with black outline are the real values of  $K_c$ . Low: signed error ( $\text{Real } K_c - \text{Pred } K_c$ )

## 4.2 Conditional simulations

We present here the results of 100 conditional simulations for time  $T$ ,  $(T + 1)$  and  $(T + 2)$ . We consider a subset of stations that are located along the direction of the advection direction, i.e. the stations represented in red in the first panel of Figure 6. Then we represent the real  $K_c$ , the mean of the predicted  $K_c$  over 10 simulations, along with a  $\pm 2\sigma$  envelope, where  $\sigma^2$  is the kriging variance among the simulations. The results for time steps  $T$ ,  $(T + 1)$  and  $(T + 2)$  are shown in the last three panels of Figure 6. We remark that the kriging variance is very small at time  $T$  and that the predicted values almost lie on the exact values; at time  $(T + 1)$  and  $(T + 2)$  the variance is larger, but all the exact values lie in the  $\pm 2\sigma$  envelope.

## 5 Discussion

The spatio-temporal SPDE approach based on advection-diffusion equations proposed in this work combines elements of physics, numerical analysis and

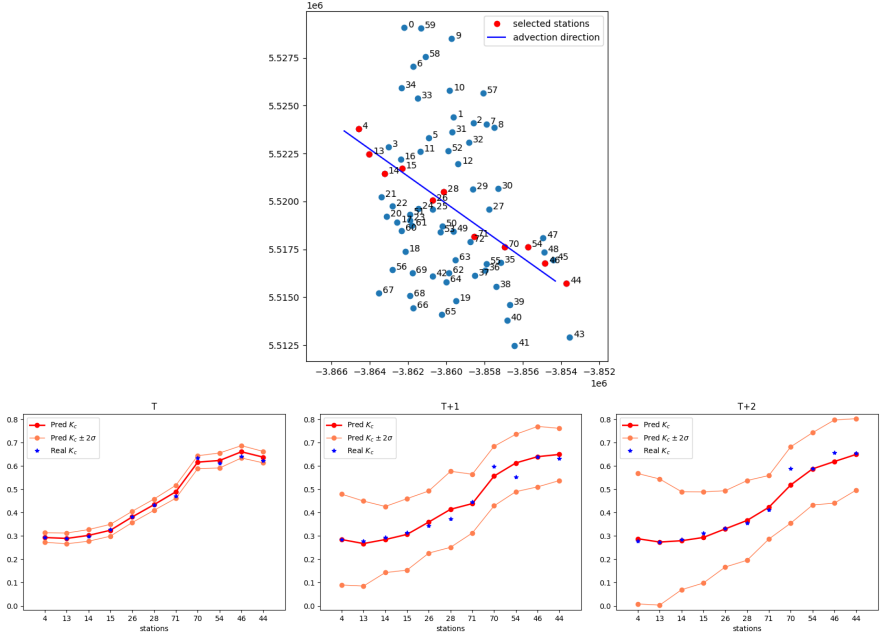


**Fig. 6** Up: Stations with estimated advection direction. Down: Real  $K_c$ , mean of predicted  $K_c$  and  $\pm 2\sigma$  envelope at time  $T$ ,  $(T + 1)$  and  $(T + 2)$

statistics. It can be seen as a first step toward *physics informed geostatistics*, which introduces physical dynamics into the statistical model, accounting for possible hidden structures governing the evolution of the spatio-temporal phenomenon. The different terms of the SPDE (advection, diffusion) directly influence the spatio-temporal dependencies of the process, by controlling its variability in space and time. Compared to spatio-temporal models built on covariance functions such as the Gneiting class (Gneiting, 2002), we gain in interpretability since the parameters of the model can be directly linked to the physical coefficients of SPDEs.

We showed that it is possible to build an accurate space-time approximations of the process driven by the SPDE using a combination of FEM in space and implicit Euler scheme in time. It leads to sparse structured linear systems. We obtained promising results for the estimation and for the prediction of processes both in terms of precision and speed. When the size of the data set is moderate, direct matrix implementation is possible. We showed how matrix-free methods can be implemented in order to obtain scalable computations even for very large datasets.

Further work would be necessary to better assess the prediction accuracy and the computational complexity. Applications to larger and more complex datasets should be considered and comparison to models expressing the advection in a Lagrangian framework (Ailliot et al., 2011; Salvaña and Genton, 2021) should be performed.

One of the main advantages of the SPDE formulation is that it is easy to generalize to non-stationary settings. Non-stationary fields can be defined by letting the parameters  $(\kappa(\mathbf{s}, t), \mathbf{v}(\mathbf{s}, t))$  be space-time-dependent. This generalization implies only minimal changes to the method used in the stationary case concerning the simulation, but needs more work for estimation and prediction, since the maximum likelihood approach becomes much more expensive. We can also incorporate models of spatially varying anisotropy by modifying the general operator  $\nabla \cdot \mathbf{H}(\mathbf{s}, t) \nabla X(\mathbf{s}, t)$  with a non-stationary anisotropic matrix  $\mathbf{H}(\mathbf{s}, t)$ . The introduction of non-stationarities could allow to better describe phenomena where local variations are clearly present. The generalization of the approaches by [Fuglstad et al. \(2015\)](#) and [Pereira \(2019\)](#) should be investigated and generalized to the spatio-temporal framework.

Another interesting consequence of defining the models through local stochastic partial differential equations is that the SPDEs still make sense when  $\mathbb{R}^d$  is replaced by a space that is only locally flat. We can define non-stationary Gaussian fields on manifolds, and still obtain a GMRF representation. Important improvements were obtained in the spatial case ([Pereira et al., 2022](#)). The generalization to space-time processes could be explored further.

Possible generalization to spatio-temporal SPDEs with a fractional exponent in the diffusion term could also be considered. A development of the methods proposed by [Bolin and Kirchner \(2020\)](#) and [Vabishchevich \(2015\)](#) should be explored.

**Acknowledgments.** We are grateful to O.I.E. center of Mines Paris – ARMINES, especially to Yves-Marie Saint-Drenan, Philippe Blanc and Hadrien Verbois, for providing the data and for inspiring discussions about renewable resources evaluation. In addition, we thank the Mines Paris / INRAE chair “Geolearning” for the constant support.

## References

- Ailliot, P., Baxelevani, A., Cuzol, A., Monbet, V., and Raillard, N. (2011). Space-time models for moving fields with an application to significant wave height fields. *Environmetrics*, 22(3):354–369.
- Bakka, H. (2018). How to solve the stochastic partial differential equation that gives a matérn random field using the finite element method.
- Bakka, H., Krainski, E., Bolin, D., Rue, H., and Lindgren, F. (2020). The diffusion-based extension of the matérn field to space-time.
- Banerjee, S., Carlin, B. P., and Gelfand, A. E. (2014). *Hierarchical Modeling and Analysis for Spatial Data (2nd ed.)*. Chapman & Hall/CRC Press. Boca Raton, FL.
- Bank, R. E., Bürgler, J. F., Fichtner, W., and Smith, R. K. (1990). Some upwinding techniques for finite element approximations of convection-diffusion equations. *Numerische Mathematik*, 58(1):185–202.

- Beyer, H. G., Costanzo, C., and Heinemann, D. (1996). Modifications of the heliosat procedure for irradiance estimates from satellite images. *Solar Energy*, 56(3):207–212.
- Bolin, D. and Kirchner, K. (2020). The rational spde approach for gaussian random fields with general smoothness. *Journal of Computational and Graphical Statistics*, 29(2):274–285.
- Cameletti, M., Lindgren, F., Simpson, D., and Rue, H. (2011). Spatio-temporal modeling of particulate matter concentration through the spde approach. *ASTA Advances in Statistical Analysis*, 97.
- Carrizo-Vergara, R., Allard, D., and Desassis, N. (2022). A general framework for spde-based stationary random fields. *Bernoulli*, 28(1):1–32.
- Chen, W., Genton, M. G., and Sun, Y. (2021). Space-time covariance structures and models. *Annual Review of Statistics and Its Application*, 8(1):191–215.
- Cressie, N. and Huang, H.-C. (1999). Classes of nonseparable, spatio-temporal stationary covariance functions. *Journal of the American Statistical Association*, 94(448):1330–1340.
- Cressie, N. and Wikle, C. K. (2011). *Statistics for Spatio-Temporal Data*. Wiley.
- Erisman, A. M. and Tinney, W. F. (1975). On computing certain elements of the inverse of a sparse matrix. *Commun. ACM*, 18(3):177–179.
- Fuglstad, G.-A., Simpson, D., Lindgren, F., and Rue, H. (2015). Does non-stationary spatial data always require non-stationary random fields? *Spatial Statistics*, 14(Part C):505–531.
- Gneiting, T. (2002). Nonseparable, stationary covariance functions for space-time data. *Journal of the American Statistical Association*, 97(458):590–600.
- Gschwind, B., Wald, L., Blanc, P., Lefèvre, M., Schroedter-Homscheidt, M., and Arola, A. (2019). Improving the mccler model estimating the downwelling solar radiation at ground level in cloud-free conditions - mccler-v3. *Meteorologische Zeitschrift*, 28(2):147–163.
- Havard Rue, L. H. (2005). *Gaussian Markov random fields: theory and applications*. Monographs on statistics and applied probability 104. Chapman & Hall/CRC, 1 edition.
- Hughes, T. and Brooks, A. (1981). A multidimensional upwind scheme with no crosswind diffusion. *Analytical and Numerical Approaches to Asymptotic Problems in Analysis*, pages 99–116.
- Hutchinson, M. (1990). A stochastic estimator of the trace of the influence matrix for laplacian smoothing splines. *Communications in Statistics - Simulation and Computation*, 19(2):433–450.
- Krainski, E., Gómez Rubio, V., Bakka, H., Lenzi, A., Castro-Camilo, D., Simpson, D., Lindgren, F., and Rue, H. (2018). *Advanced Spatial Modeling with Stochastic Partial Differential Equations Using R and INLA*. Chapman & Hall/CRC Press. Boca Raton, FL.
- Lindgren, F., Bolin, D., and Rue, H. (2022). The spde approach for gaussian and non-gaussian fields: 10 years and still running. *Spatial Statistics*,

- 50:100599. Special Issue: The Impact of Spatial Statistics.
- Lindgren, F. and Rue, H. (2015). Bayesian spatial modelling with r-inla. *Journal of Statistical Software*, 63(19):1–25.
- Lindgren, F., Rue, H., and Lindström, J. (2011). An explicit link between gaussian fields and gaussian markov random fields: the stochastic partial differential equation approach. *Journal of the Royal Statistical Society: Series B (Statistical Methodology)*, 73(4):423–498.
- Liu, X., Yeo, K., and Lu, S. (2020). Statistical modeling for spatio-temporal data from stochastic convection-diffusion processes. *Journal of the American Statistical Association*, pages 1–37.
- Macke, A., Seifert, P., Baars, H., Barthlott, C., Beekmans, C., Behrendt, A., Bohn, B., Brueck, M., Bühl, J., Crewell, S., Damian, T., Deneke, H., Düsing, S., Foth, A., Di Girolamo, P., Hammann, E., Heinze, R., Hirsikko, A., Kalisch, J., Kalthoff, N., Kinne, S., Kohler, M., Löhnert, U., Madhavan, B. L., Maurer, V., Muppa, S. K., Schween, J., Serikov, I., Siebert, H., Simmer, C., Späth, F., Steinke, S., Trümner, K., Trömel, S., Wehner, B., Wieser, A., Wulfmeyer, V., and Xie, X. (2017). The hd(cp)<sup>2</sup> observational prototype experiment (hope) – an overview. *Atmospheric Chemistry and Physics*, 17(7):4887–4914.
- Mekuria, G. and Rao, J. (2016). Adaptive finite element method for steady convection-diffusion equation. *American Journal of Computational Mathematics*, 06:275–285.
- Oumbe, A., Qu, Z., Blanc, P., Lefèvre, M., Wald, L., and Cros, S. (2014). Decoupling the effects of clear atmosphere and clouds to simplify calculations of the broadband solar irradiance at ground level. *Geoscientific Model Development*, 7(4):1661–1669.
- Pereira, M. (2019). *Generalized random fields on Riemannian manifolds : theory and practice*. PhD thesis, Mines Paris, PSL University.
- Pereira, M. and Desassis, N. (2019). Efficient simulation of gaussian markov random fields by chebyshev polynomial approximation. *Spatial Statistics*, 31:100359.
- Pereira, M., Desassis, N., and Allard, D. (2022). Geostatistics for large datasets on Riemannian manifolds: a matrix-free approach. working paper or preprint.
- Porcu, E., Furrer, R., and Nychka, D. (2021). 30 years of space–time covariance functions. *Wiley Interdisciplinary Reviews: Computational Statistics*, 13(2):e1512.
- Powell, P. (2011). Calculating determinants of block matrices.
- Quarteroni, A. (2008). *Modellistica Numerica per Problemi Differenziali*. Springer Milano.
- Roques, L., Allard, D., and Soubeyrand, S. (2022). Spatial statistics and stochastic partial differential equations: A mechanistic viewpoint. *Spatial Statistics*, 50:100591.
- Salvaña, M. L. O. and Genton, M. G. (2021). *Lagrangian Spatio-Temporal Nonstationary Covariance Functions*, pages 427–447. Springer International

Publishing, Cham.

- Schade, N. H., Macke, A., Sandmann, H., and Stick, C. (2007). Enhanced solar global irradiance during cloudy sky conditions. *Meteorologische Zeitschrift*, 16:295–303.
- Sigrist, F., Künsch, H. R., and Stahel, W. A. (2012). A dynamic nonstationary spatio-temporal model for short term prediction of precipitation. *The Annals of Applied Statistics*, 6(4).
- Sigrist, F., Künsch, H. R., and Stahel, W. A. (2015). Stochastic partial differential equation based modelling of large space-time data sets. *Journal of the Royal Statistical Society: Series B (Statistical Methodology)*, 77(1):3–33.
- Stein, M. L. (2005). Space-time covariance functions. *Journal of the American Statistical Association*, 100(469):310–321.
- Takahashi, K., Fagan, J., and Chin, M. (1973). Formation of a sparse bus impedance matrix and its application to short circuit study. 8th PICA Conf. Proc. June 4-6, Minneapolis, Minn.
- Vabishchevich, P. N. (2015). Numerically solving an equation for fractional powers of elliptic operators. *Journal of Computational Physics*, 282:289–302.
- Whittle, P. (1954). On stationary processes in the plane. *Biometrika*, 41(3-4):434–449.
- Whittle, P. (1963). Stochastic processes in several dimensions. *Bull. Inst. Int. Statist.*, 40:974–994.
- Wikle, C. and Hooten, M. (2010). A general science-based framework for dynamical spatio-temporal models. *TEST*, 19:417–451.
- Wikle, C. K. and Cressie, N. (1999). A dimension-reduced approach to space-time kalman filtering. *Biometrika*, 86(4):815–829.

## Appendix A Discretization of spatio-temporal advection-diffusion SPDE

We here prove the discretization scheme of the advection-diffusion spatio-temporal SPDE (4). For the sake of a clearer exposition, we have been set  $\mathbf{H} = \mathbf{I}$ ,  $\alpha = 1$  and the spatio-temporal noise  $Z(\mathbf{s}, t)$  has been set to a spatio-temporal white noise  $W(\mathbf{s}, t)$ . The proof for the general case follows exactly the same lines as the proof below. The considered SPDE is

$$\left[ \frac{\partial}{\partial t} + \frac{1}{c}(\kappa^2 - \Delta) + \frac{1}{c} \boldsymbol{\gamma} \cdot \nabla \right] X(\mathbf{s}, t) = \frac{\tau}{\sqrt{c}} W(\mathbf{s}, t). \quad (\text{A1})$$

For the discretization of the temporal derivative in Equation (A1), we opt for the implicit Euler scheme, which considers the differential equation

$$\frac{\partial X}{\partial t} = f(t, X),$$

with initial value  $X(t_0) = X_0$ , where both the function  $f$  and the initial data  $t_0$  and  $X_0$  are known; the function  $X$  depends on the real variable  $t$  and is unknown. The method produces a sequence  $X_0, X_1, X_2, \dots$ , such that  $X_k$  approximates  $X(t_0 + kdt)$ , where  $dt$  is the time step size. The approximation reads

$$X_{k+1} = X_k + dt f(t_{k+1}, X_{k+1}).$$

In the specific case of Equation (A1), the implicit Euler discretization step reads

$$X(\mathbf{s}, t+dt) - X(\mathbf{s}, t) + dt \left[ \frac{1}{c}(\kappa^2 - \Delta) + \frac{1}{c} \boldsymbol{\gamma} \cdot \nabla \right] X(\mathbf{s}, t+dt) = \frac{\sqrt{dt}\tau}{\sqrt{c}} W_{S,t+dt}(\mathbf{s}), \quad (\text{A2})$$

where  $W_{S,t+dt}(\mathbf{s})$  is a spatial white noise. For ease of notation, we define  $x = X(\mathbf{s}, t+dt)$  the unknown variable, that is defined with respect to  $x_t = X(\mathbf{s}, t)$ .

At each time step of the temporal discretization a spatial discretization method is applied. In our case, we use the Finite Element Method called Continuous Galerkin with Neumann boundary condition. The weak form of Equation (A2) is

$$\int_{\Omega} x v d\mathbf{s} + \frac{dt}{c} \left( \int_{\Omega} \kappa^2 x v d\mathbf{s} - \int_{\Omega} \Delta x v d\mathbf{s} + \int_{\Omega} \boldsymbol{\gamma} \cdot \nabla x v d\mathbf{s} \right) = \int_{\Omega} x_t v d\mathbf{s} + \frac{\sqrt{dt}\tau}{\sqrt{c}} \int_{\Omega} v dW(\mathbf{s}), \quad \forall v \in \mathcal{V},$$

where  $\mathcal{V}$  is the space of the solutions.

By applying Green's first identity (i.e. by writing  $\int_{\Omega} \Delta x v d\mathbf{s} = - \int_{\Omega} \nabla x \cdot \nabla v d\mathbf{s} + \int_{\partial\Omega} v \cdot (\nabla x \cdot \hat{\mathbf{n}}) d\sigma$ , with  $\hat{\mathbf{n}}$  being the normal vector on the boundary)

and simplifying the second term thanks to the Neumann boundary condition, we obtain

$$\begin{aligned} & \underbrace{\int_{\Omega} xvd\mathbf{s} + \frac{dt}{c} \left( \int_{\Omega} \kappa^2 xvd\mathbf{s} + \int_{\Omega} \nabla x \cdot \nabla vd\mathbf{s} + \int_{\Omega} \gamma \cdot \nabla xvd\mathbf{s} \right)}_{\mathcal{A}(x,v)} \\ &= \underbrace{\int_{\Omega} x_tv d\mathbf{s}}_{\mathcal{C}(x_t,v)} + \underbrace{\frac{\sqrt{dt}\tau}{\sqrt{c}} \int_{\Omega} vdW(\mathbf{s})}_{\mathcal{E}(v)}, \quad \forall v \in \mathcal{V}. \end{aligned}$$

The generalized Galerkin method allows us to find an approximated solution  $x_h \in \mathcal{V}_h \subseteq \mathcal{V}$  to the SPDE, with  $\mathcal{V}_h$  being the space of finite element solutions, such that

$$\mathcal{A}(x_h, v_h) = \mathcal{C}(x_{t,h}, v_h) + \mathcal{E}(v_h) \quad \forall v_h \in \mathcal{V}_h.$$

We now write the functions  $x_h$ ,  $x_{t,h}$  and  $v_h$  as linear combination of the basis hat functions  $\{\psi_i\}_{i=1}^{N_S}$  defined over the triangulation of the spatial domain and the weight functions  $\{x_{h,i}\}_{i=1}^{N_S}$ ,  $\{x_{t,h,i}\}_{i=1}^{N_S}$  and  $\{v_{h,i}\}_{i=1}^{N_S}$ :

$$x_h = \sum_i^{N_S} x_{h,i} \psi_i; \quad x_{t,h} = \sum_i^{N_S} x_{t,h,i} \psi_i; \quad v_h = \sum_i^{N_S} v_{h,i} \psi_i.$$

Because of the linearity in the first argument of  $\mathcal{A}(\cdot, \cdot)$  and  $\mathcal{C}(\cdot, \cdot)$ , we obtain

$$\sum_i^{N_S} \mathcal{A}(\psi_i, v_h) x_{h,i} = \sum_i^{N_S} \mathcal{C}(\psi_i, v_h) x_{t,h,i} + \mathcal{E}(v_h), \quad \forall v_h \in \mathcal{V}_h, \quad (\text{A3})$$

where

$$\begin{aligned} \mathcal{A}(\psi_i, v_h) &= \mathcal{M}(\psi_i, v_h) + \frac{dt}{c} (\mathcal{K}(\psi_i, v_h) + \mathcal{B}(\psi_i, v_h)) \\ \mathcal{C}(\psi_i, v_h) &= \mathcal{M}(\psi_i, v_h), \end{aligned}$$

with  $\mathcal{K}(\psi_j, v_h) = \kappa^2 \mathcal{M}(\psi_j, v_h) + \mathcal{G}(\psi_j, v_h)$ . Here,  $\mathcal{M}$  and  $\mathcal{G}$  are the mass and stiffness operators, respectively  $\mathcal{M}(v, w) = \int_{\Omega} vwd\mathbf{s}$  and  $\mathcal{G}(v, w) = \int_{\Omega} \nabla v \cdot \nabla wd\mathbf{s}$ .  $\mathcal{B}$  is the advection operator, i.e.,  $\mathcal{B}(v, w) = \int_{\Omega} \gamma \cdot \nabla vwd\mathbf{s}$ . Finally,  $\mathcal{E}$  is the operator of the form  $\mathcal{E}(v) = \frac{\sqrt{dt}\tau}{\sqrt{c}} \int_{\Omega} vdW\mathbf{s}$ .

Since any  $v_h$  can be written as a linear combination of basis functions, the formulation (A3) is equivalent to

$$\sum_i^{N_S} \mathcal{A}(\psi_i, \psi_j) x_{h,i} = \sum_i^{N_S} \mathcal{C}(\psi_i, \psi_j) x_{t,h,i} + \mathcal{E}(\psi_j), \quad \forall j \quad (\text{A4})$$

We define  $\mathbf{M} = [M_{ij}]_{i,j=1}^{N_S} = [\mathcal{M}(\psi_i, \psi_j)]_{i,j=1}^{N_S}$ ,  $\mathbf{G} = [G_{ij}]_{i,j=1}^{N_S} = [\mathcal{G}(\psi_i, \psi_j)]_{i,j=1}^{N_S}$ ,  $\mathbf{B} = [B_{ij}]_{i,j=1}^{N_S} = [\mathcal{B}(\psi_i, \psi_j)]_{i,j=1}^{N_S}$  the mass, stiffness and advection matrices, respectively.  $\mathcal{E}(\psi_j)$  is a random variable with 0-expectation and covariance equal to

$$\begin{aligned} \text{Cov}(\mathcal{E}(\psi_i), \mathcal{E}(\psi_j)) &= \frac{dt\tau^2}{c} \text{Cov} \left( \int_{\Omega} \psi_i dW \mathbf{s}, \int_{\Omega} \psi_j dW \mathbf{s} \right) \\ &= \frac{dt\tau^2}{c} \int_{\Omega} \psi_i \psi_j d\mathbf{s} = \frac{dt\tau^2}{c} M_{ij}. \end{aligned}$$

If  $\mathbf{z}_t$  is a  $(N_S)$ -Gaussian vector such that  $\mathbf{z}_t \sim \mathcal{N}(\mathbf{0}, \mathbf{I})$ ,  $\mathbf{x}_{t+dt}$  is the vector containing the values  $\{x_{h,i}\}_{i=1}^{N_S}$  and  $\mathbf{x}_t$  is the vector containing the values  $\{x_{t,h,i}\}_{i=1}^{N_S}$ , then the sparse linear system corresponding to Equation (A4) reads

$$\mathbf{M} \mathbf{x}_{t+dt} + \frac{dt}{c} (\mathbf{K} + \mathbf{B}) \mathbf{x}_{t+dt} = \mathbf{M} \mathbf{x}_t + \frac{\sqrt{dt}\tau}{\sqrt{c}} \mathbf{M}^{1/2} \mathbf{z}_t, \quad (\text{A5})$$

where  $\mathbf{K} = \kappa^2 \mathbf{M} + \mathbf{G}$ .

## Appendix B Advection-dominated SPDE

The stabilization of advection-dominated SPDEs is made through the introduction of a stabilization term that has the purpose of eliminating, or at least reducing, the numerical oscillations produced by the Galerkin method (when the grid is not fine enough). This term has to vanish in the limit  $h \rightarrow 0$  to ensure consistency.

In the simplified case of a 1D Partial Differential Equation with diffusion and advection terms

$$-\nabla \cdot \lambda \nabla u + \gamma \cdot \nabla u = f,$$

a way of stabilizing the advection operator  $\gamma \cdot \nabla$  is to replace the diffusion coefficient  $\lambda$  with  $\tilde{\lambda} = \lambda(1 + \phi(\text{Pe}_h))$ , where  $\text{Pe}_h$  is the Péclet number defined in Section 2.4 and  $\lim_{h \rightarrow 0} \phi(\text{Pe}_h) = 0$ . A clear explanation of this method is detailed in Chapter 5 of Quarteroni (2008). The method is called *upwind* (U) in the simplified case where  $\phi(\text{Pe}_h) = \text{Pe}_h$ . The idea behind the stabilization method is to add an artificial diffusion term equal to  $\nabla \cdot \lambda \phi(\text{Pe}_h) \nabla u$  that depends on the size of the discretization mesh  $h$  and on the Péclet number. In this way, the equation with the additional stabilization term

$$-\nabla \cdot \lambda(1 + \phi(\text{Pe}_h)) \nabla u + \gamma \cdot \nabla u = f$$

is no more advection-dominated since its Péclet number  $\tilde{\text{Pe}}_h$  is now equal to

$$\tilde{\text{Pe}}_h = \frac{\text{Pe}_h}{1 + \phi(\text{Pe}_h)}$$

and always satisfies  $\tilde{\text{Pe}}_h < 1$ .

The extension of the 1D upwind stabilization model to dimension  $d = 2$  is obtained by adding to the bilinear form  $\mathcal{A}$  defined in Appendix A the stabilization term  $\mathcal{S}_U$  such that

$$\mathcal{S}_U(u_h, v_h) = Qh \int_{\Omega} \nabla u_h \cdot \nabla v_h d\mathbf{s}, \quad Q > 0. \quad (\text{B6})$$

This stabilization term can be considered as an additional artificial diffusion equal to  $Qh\Delta X(\mathbf{s}, t)$  in SPDE (4). This diffusion is not only on the direction of the transport, where we aim to reduce the oscillations, but also on the orthogonal direction, where there is no problem of convergence. For this reason, we use a different stabilization method, called *Streamline Diffusion* method (SD) (Hughes and Brooks, 1981), that considers only an artificial diffusion along the advection direction by adding in the left-hand side of SPDE (4) the term

$$\mathcal{S}_{SD}(u_h, v_h) = \frac{h}{|\boldsymbol{\gamma}|} \int_{\Omega} (\boldsymbol{\gamma} \cdot \nabla u_h)(\boldsymbol{\gamma} \cdot \nabla v_h) d\mathbf{s}. \quad (\text{B7})$$

It's worth noticing that in both the stabilization terms (B6) and (B7) the scaling coefficient  $h$  has been introduced to recover consistency. Both methods are only weakly consistent and provide an error that is  $\mathcal{O}(h)$  if finite element are used (first order convergent). In our work, we opt for the Streamline Diffusion method and define  $\mathcal{S} = \mathcal{S}_{SD}$  for ease of notation.

## Appendix C Proof of global precision matrix

We present here the proof of Proposition 6. By calling  $\mathbf{x}_{0:t} = [\mathbf{x}_0, \dots, \mathbf{x}_t]^\top$  the vector containing all spatial solutions until time step  $t$  we can write

$$\mathbf{x}_{0:t} = \mathbf{R} \begin{pmatrix} \mathbf{x}_0 \\ \mathbf{z}_{0:t} \end{pmatrix},$$

with  $\mathbf{z}_{0:t} = [\mathbf{z}_1, \dots, \mathbf{z}_t]^\top$  and

$$\mathbf{R} = \begin{pmatrix} \mathbf{I} & 0 & 0 & 0 & \dots & 0 \\ \mathbf{D} & \mathbf{E} & 0 & 0 & \dots & 0 \\ \mathbf{D}^2 & \mathbf{D}\mathbf{E} & \mathbf{E} & 0 & \dots & 0 \\ \vdots & \ddots & \ddots & \ddots & \ddots & \vdots \\ \vdots & \ddots & \ddots & \ddots & \ddots & 0 \\ \vdots & \ddots & \ddots & \mathbf{D}^2 & \mathbf{D} & \mathbf{E} \end{pmatrix}.$$

$\mathbf{R}$  has a block structure which allows easy computation of its inverse

$$\mathbf{R}^{-1} = \begin{pmatrix} \mathbf{I} & 0 & 0 & 0 & \dots & 0 \\ -\mathbf{E}^{-1} \mathbf{D} & \mathbf{E}^{-1} & 0 & 0 & \dots & 0 \\ 0 & -\mathbf{E}^{-1} \mathbf{D} \mathbf{E}^{-1} & 0 & \dots & 0 \\ \vdots & \ddots & \ddots & \ddots & \ddots & \vdots \\ \vdots & \ddots & \ddots & \ddots & \ddots & 0 \\ 0 & \dots & \dots & 0 & -\mathbf{E}^{-1} \mathbf{D} \mathbf{D}^{-1} \end{pmatrix}.$$

The precision matrix of  $\mathbf{x}_{0:t}$  is thus

$$\mathbf{Q} = \mathbf{R}^{-1\top} \begin{pmatrix} \Sigma_0^{-1} & 0 & \dots & 0 \\ 0 & \mathbf{I} & \dots & 0 \\ \vdots & \ddots & \ddots & \vdots \\ 0 & 0 & \dots & \mathbf{I} \end{pmatrix} \mathbf{R}^{-1}.$$

By denoting  $\mathbf{F} = \mathbf{E} \mathbf{E}^\top$ , the global precision matrix reads

$$\mathbf{Q} = \begin{pmatrix} \Sigma_0^{-1} + \mathbf{D}^\top \mathbf{F}^{-1} \mathbf{D} & -\mathbf{D}^\top \mathbf{F}^{-1} & 0 & \dots & 0 \\ -\mathbf{F}^{-1} \mathbf{D} & \mathbf{F}^{-1} + \mathbf{D}^\top \mathbf{F}^{-1} \mathbf{D} & -\mathbf{D}^\top \mathbf{F}^{-1} & \ddots & \vdots \\ \vdots & \ddots & \ddots & \ddots & 0 \\ \vdots & \ddots & -\mathbf{F}^{-1} \mathbf{D} & \mathbf{F}^{-1} + \mathbf{D}^\top \mathbf{F}^{-1} \mathbf{D} & -\mathbf{D}^\top \mathbf{F}^{-1} \\ 0 & \dots & 0 & -\mathbf{F}^{-1} \mathbf{D} & \mathbf{F}^{-1} \end{pmatrix}.$$

## Appendix D Matrix-free approach for solving systems

In computational mathematics, a matrix-free method is an algorithm for solving a linear system of equations that does not store the coefficient matrix explicitly, but accesses the matrix by evaluating matrix-vector products. Such methods can be preferable when the matrix is so big that storing and manipulating it would cost a lot of memory and computing time, even with the use of methods for sparse matrices. Many iterative methods allow for a matrix-free implementation, including the Conjugate Gradient method.

### D.1 Conjugate Gradient method

Suppose we want to solve the system of linear equations

$$\mathbf{A} \mathbf{x} = \mathbf{b}$$

for the vector  $\mathbf{x}$ , where the known  $(n, n)$  matrix  $\mathbf{A}$  is symmetric, positive-definite, and real, and  $\mathbf{b}$  is known as well. We denote the unique solution of this

system by  $\mathbf{x}^*$ . The Conjugate Gradient (CG) method is an iterative method that allows us to approximately solve systems where  $n$  is so large that the direct method would take too much time.

We denote the initial guess for  $\mathbf{x}^*$  by  $\mathbf{x}_0$  (without loss of generality  $\mathbf{x}_0 = 0$ ). Starting with  $\mathbf{x}_0$ , at each iteration we need a metric to tell us whether we are closer to the solution  $\mathbf{x}^*$ . This metric comes from the fact that the solution  $\mathbf{x}^*$  is also the unique minimizer of the following quadratic function

$$f(\mathbf{x}) = \frac{1}{2} \mathbf{x}^\top \mathbf{A} \mathbf{x} - \mathbf{x}^\top \mathbf{b}, \quad \mathbf{x} \in \mathbf{R}^n,$$

The existence of a unique minimizer is guaranteed by the fact that the Hessian matrix of  $f$  is symmetric positive-definite  $\mathbf{H}(f(\mathbf{x})) = \mathbf{A}$ , and that the minimizer solves the initial problem, since  $\nabla f(\mathbf{x}) = \mathbf{A} \mathbf{x} - \mathbf{b}$ .

We take the first basis vector  $\mathbf{p}_0$  to be the negative of the gradient of  $f$  at  $\mathbf{x} = \mathbf{x}_0$ , leading to  $\mathbf{p}_0 = \mathbf{b} - \mathbf{A} \mathbf{x}_0$ . The other vectors in the basis will be conjugate to the gradient. Note that  $\mathbf{p}_0$  is also the residual  $\mathbf{r}_0$  provided by this initial step of the algorithm. In fact,  $\mathbf{r}_k$  is such that  $\mathbf{r}_k = \mathbf{b} - \mathbf{A} \mathbf{x}_k$ . The directions  $\mathbf{p}_k$  has to be conjugate to each other. To enforce this condition, we require the next search direction to be built out of the current residual and all previous search directions. The conjugation constraint is an orthonormal-type constraint, which makes the algorithm an example of Gram-Schmidt orthonormalization. This gives the expression

$$\mathbf{p}_k = \mathbf{r}_k - \sum_{i < k} \frac{\mathbf{p}_i^\top \mathbf{A} \mathbf{r}_k}{\mathbf{p}_i^\top \mathbf{A} \mathbf{p}_i} \mathbf{p}_i.$$

Following this direction, the next optimal location is given by

$$\mathbf{x}_{k+1} = \mathbf{x}_k + \alpha_k \mathbf{p}_k,$$

with

$$\alpha_k = \frac{\mathbf{p}_k^\top (\mathbf{b} - \mathbf{A} \mathbf{x}_k)}{\mathbf{p}_k^\top \mathbf{A} \mathbf{p}_k} = \frac{\mathbf{p}_k^\top \mathbf{r}_k}{\mathbf{p}_k^\top \mathbf{A} \mathbf{p}_k}.$$

The expression for  $\alpha_k$  can be derived if one substitutes the expression for  $\mathbf{x}_{k+1}$  into  $f$  and minimizes it w.r.t.  $\alpha_k$ :

$$\begin{aligned} f(\mathbf{x}_{k+1}) &= f(\mathbf{x}_k + \alpha_k \mathbf{p}_k) = g(\alpha_k) \\ g'(\alpha_k) &\neq 0 \Rightarrow \alpha_k = \frac{\mathbf{p}_k^\top (\mathbf{b} - \mathbf{A} \mathbf{x}_k)}{\mathbf{p}_k^\top \mathbf{A} \mathbf{p}_k}. \end{aligned}$$

The algorithm seems to require storage of all previous searching directions and residual vectors, as well as many matrix-vector multiplications, leading to expensive computations. However, a closer analysis of the algorithm shows that  $\mathbf{r}_i$  is orthogonal to  $\mathbf{r}_j$ , i.e.  $\mathbf{r}_i^\top \mathbf{r}_j = 0$  for  $i \neq j$ , and  $\mathbf{p}_i$  is  $\mathbf{A}$ -orthogonal to

$\mathbf{p}_j$ , i.e.  $\mathbf{p}_i^\top \mathbf{A} \mathbf{p}_j = 0$  for  $i \neq j$ . This means that, as the algorithm progresses,  $\mathbf{p}_i$  and  $\mathbf{r}_i$  span the same Krylov subspace.  $\{\mathbf{r}_i\}$  form the orthogonal basis with respect to the standard inner product, and  $\{\mathbf{p}_i\}$  form the orthogonal basis with respect to the inner product induced by  $\mathbf{A}$ . Therefore,  $\mathbf{x}_k$  can be regarded as the projection of  $\mathbf{x}$  on the Krylov subspace.

## D.2 Gauss-Seidel preconditioner

The general concept behind a preconditioner is the following: given a linear system  $\mathbf{A} \mathbf{x} = \mathbf{b}$ , we want to find the matrix  $\mathbf{P}_R$  and/or  $\mathbf{P}_L$  such that the condition number of  $\mathbf{A} \mathbf{P}_R^{-1}$  (right preconditioner) or  $\mathbf{P}_L^{-1} \mathbf{A}$  (left preconditioner) or  $\mathbf{P}_L^{-1} \mathbf{A} \mathbf{P}_R^{-1}$  is better than for  $\mathbf{A}$  and that we can easily solve  $\mathbf{P}_L \mathbf{y} = \mathbf{g}$  or  $\mathbf{P}_R \mathbf{y} = \mathbf{g}$  for any  $\mathbf{g}$ . Then we solve for  $\mathbf{A} \mathbf{P}_R^{-1} \mathbf{y} = \mathbf{b}$  (right preconditioner),  $\mathbf{P}_R \mathbf{x} = \mathbf{y}$  or  $\mathbf{P}_L^{-1} \mathbf{A} \mathbf{x} = \mathbf{P}_L^{-1} \mathbf{b}$  (left preconditioner) or even both  $\mathbf{P}_L^{-1} \mathbf{A} \mathbf{P}_R^{-1} \mathbf{y} = \mathbf{P}_L^{-1} \mathbf{b}$ ,  $\mathbf{P}_R \mathbf{x} = \mathbf{y}$ .

The best choice is of course  $\mathbf{P} = \mathbf{A}$ , but this does not make life easier. One of the ideas is to use other iterative methods as preconditioners, such as the Jacobi method, the Gauss-Seidel method or the  $\text{SOR}(\omega)$  method (Successive over-relaxation).

A well-known method is Gauss-Seidel (GS) method, whose matrix form is here detailed. Given the matrix  $\mathbf{A}$ , we have

$$\mathbf{A} = \mathbf{L} + \mathbf{D} + \mathbf{L}^*,$$

where  $\mathbf{D}$  is the diagonal of  $\mathbf{A}$ ,  $\mathbf{L}$  is lower-triangular part with zero on the diagonal. One iteration of the GS method reads

$$\mathbf{x}_{k+1} = \mathbf{x}_k - (\mathbf{L} + \mathbf{D})^{-1} (\mathbf{A} \mathbf{x}_k - \mathbf{b})$$

and we refer to the preconditioner  $\mathbf{P} = \mathbf{L} + \mathbf{D}$  as Gauss-Seidel preconditioner. A good property of this preconditioner is that  $\rho(\mathbf{I} - (\mathbf{L} + \mathbf{D})^{-1} \mathbf{A}) < 1$ , where  $\rho$  is the spectral radius, i.e., for a positive definite matrix GS-method always converges.